Geothermics 133 (2025) 103475

Contents lists available at ScienceDirect

Geothermics

journal homepage: www.elsevier.com/locate/geothermics

Life cycle assessment of two deep geothermal heating plants and the potential of auxiliary energy to reduce environmental burden

Hannah Uhrmann *, Florian Heberle, Dieter Brüggemann

Center of Energy Technology (ZET), University of Bayreuth, Prof.-Rüdiger-Bormann-Strasse 1, 95440, Bayreuth, Germany

ARTICLE INFO

Keywords:
Geothermal heating plant
Life cycle assessment
Peak load and redundancy coverage
Electricity mix
Biomethane

ABSTRACT

Geothermal energy is promising as a low-carbon alternative for heat generation. This paper presents a life cycle assessment (LCA) of two currently operational deep geothermal plants in the Southern German Molasse Basin according to ISO 14040 and 14044. The plants significantly differ in geothermal water temperature and auxiliary energy usage. Additionally, one plant is coupled to a cogeneration unit. The environmental impact of the plants varies greatly, with 81 and 195 g CO_2 eq./kWh for global warming impact. In comparison to the typical German mix utilized for district heating in the year 2023, geothermal heat exhibits a substantial reduction potential. The primary impact of both plants is mainly attributed to the operational phase, specifically the use of auxiliary energy to meet the electricity demand of the downhole pumps. Another major contribution is the peak load and redundancy coverage. Conducting scenario analyses regarding auxiliary energy usage, it was found that switching to a more renewable electricity mix could lead to a reduction of up to 39 % in Global Warming Potential (GWP). Utilizing biomethane for peak load and redundancy coverage results in a reduction of up to 77 %. Hereby, the improvement potential significantly depends on both the type and quantity of auxiliary energy used. The findings underscore the significance of auxiliary energy in mitigating the environmental impact of deep geothermal heating facilities, which can contribute to achieving the EU's net-zero targets.

1. Introduction

To meet the objective of the IPCC and limit anthropogenic climate change, it is essential to decarbonize the heating sector. In Germany, especially, the share of renewable heat sources is considerably low, with only 18.2 % in 2022 (Lauf et al., 2023). Thereby, the average fossil district heating is dominated by natural gas (62.2 %) and hard coal (27.3 %) and therefore exhibits a high average GWP with 307.5 g CO_2 eq./kWh (Lauf et al., 2023). Hereby, geothermal energy has great potential and could substitute up to 40 % (7 655 MW) of the heat demand in the state of Bavaria (Keim et al., 2020). Therefore, the technology has also gained political interest due to the fossil fuel supply's independence. However, even with this technology, characterized by costly deep drilling, the question of how well it is compatible with the climate goals is open. The Technical Expert Group on Sustainable Finance has set a threshold of 100 g CO_2 eq./kWh for 2020. Any technology that falls at or below that threshold is considered in line with the Paris Climate Agreement (EU Technical Expert Group on Sustainable Finance, 2020). Additionally, this threshold decreases every five years until net zero in 2050. This ensures the necessity to identify strategies for reducing GWP. This study focuses on deep hydro-geothermal systems. Therefore, geothermal systems coupled with ground-source heat pumps are not discussed further here. Deep geothermal energy can generally be utilized for generating electricity, heat, and as well as cogeneration of heat and power. There have been a number of LCA studies on these systems; they are briefly discussed in the section below.

1.1. Power plants

In case of deep geothermal systems, electricity generation is already examined in several publications. In a recent review paper, Li et al. (Li et al., 2023) identified 36 studies analyzing the environmental impact of geothermal power that were published since 2000. The carbon footprint varied significantly from 3.9 for a Chinese plant with an unusually steep heat gradient (Wang et al., 2020) and up to 1040 g CO_2 eq./kWh_{el}. for an Italian plant with unstable methane emissions (Bravi and Basosi, 2014). Li et al. demonstrated which technologies and types of geothermal

* Corresponding author.
E-mail address: hannah.uhrmann@uni-bayreuth.de (H. Uhrmann).

https://doi.org/10.1016/j.geothermics.2025.103475
Received 28 April 2025; Received in revised form 3 August 2025; Accepted 13 August 2025
Available online 27 August 2025

sources are crucial for keeping the environmental impact low. Regardless of the geothermal source, ORC systems performed particularly well, with an average of 12.8 CO_2 eq./kWh, significantly falling below the taxonomy threshold. In general, a wide variety of aspects of power systems were investigated, covering the diversity of geothermal systems and influencing factors. Li et al., for example, focused on the potential of abandoned gas and oil wells and found that repurposed systems can cut carbon emissions by 34 % compared to conventional geothermal power plants (Li et al., 2024). Menberg et al. (Menberg et al., 2021) focused on influences of the operational phase, such as refrigerant use and leakage and auxiliary energy use for drilling. Whereas the use of low GWP refrigerants and electricity in place of diesel for drilling operations has been demonstrated to have a beneficial environmental impact. Heberle et al. (Heberle et al., 2016) demonstrated the importance of selecting low GWP refrigerants and effective ORC concepts, which can potentially reduce the carbon footprint by up to 80 % compared to conventional single-stage concepts and fluorinated hydrocarbons as working fluids. A minor influence on the environmental burden, however, could be attributed to the end-of-life phase of geothermal plants, according to Rossi et al. (Rossi et al., 2023), who investigated this phase specifically in comparison to the end-of-life phase of other renewable sources, photovoltaic and wind.

While aspects of the circular process, such as the use of refrigerants in electricity generation, apply only to the LCA of power plants, other parts of the findings from power plant LCAs are also relevant to heating plants. the work of Zuffi et al. (Zuffi et al., 2022) highlights the significance of closed-loop systems due to dissolved greenhouse gases in the geothermal fluid by comparing five plants in three countries. Following this, Karlsdottir et al. (Karlsdottir et al., 2020) demonstrated that reinjecting direct emissions can reduce GWP by 28 % for electricity production at the Icelandic plant Hellisheiði.

1.2. Cogeneration of heat and power

Several studies also investigated cogeneration of heat and electricity (Karlsdottir et al., 2020; Menberg et al., 2023; Paulillo et al., 2020; Pratiwi et al., 2018; Gkousis et al., 2022). Thereby, adding heat generation to the power plants can reduce the environmental burden (Paulillo et al., 2020; Pratiwi et al., 2018). In general, the environmental impact of heat generation of these cogeneration plants is relatively small: Menberg et al. (Menberg et al., 2023) analyzed various configurations for heat extraction from a two-stage organic Rankine cycle at a cogeneration plant in the Southern German Molasse Basin, resulting in a GWP of 3.9 to 4.0 g CO_2 eq/kWh. In a similar effort to reduce environmental impact, Karlsdottir et al. (Karlsdottir et al., 2020) studied an Icelandic cogeneration plant and achieved a significant reduction in GWP by reinjecting CO_2 as a method of carbon capture and storage, lowering it from 15.8 to 11.2 g CO_2 eq/kWh. Pratiwi et al. (Pratiwi et al., 2018) investigated the potential for cogeneration of heat and power as a scenario based on a future project in the Illkirch-Graffenstaden plant in France. Their findings indicated that this could result in emissions of 2.69–4.36 g CO_2 eq./kWh. This can be mainly attributed to the combined plants being able to cover their own electricity demand and thereby being independent of the electricity mix with possible high emissions.

1.3. Heating plants

Though there is an increasing number of geothermal heating plants, studies on the environmental impact of deep geothermal heating are generally underrepresented (Pratiwi and Trutnevyte, 2021). Table 1 gives an overview of the literature on LCA studies on deep hydro geothermal heating projects.

In contrast to cogeneration for sole heat generation, the supply of auxiliary energy plays a more significant role since the demand of the downhole pumps cannot be allocated with the plant's own electricity generation (Menberg et al., 2023). The used electricity mix plays a vital role in recent studies: While the French Rittershofen heating plant only results in 3.8 g CO_2 eq./kWh with the French electricity mix dominated by nuclear energy (66 % in 2020) (Douziech et al., 2021), a feasibility study for a geothermal heating plant in China leads to 187.7 g CO_2 eq./kWh[1] due to the local coal heavy mix (Zhang et al., 2020). Plants like VITO-plant in northern Belgium analyzed by Gkousis et al. (Gkousis et al., 2024) were especially depended on the electricity mix, since the rock permeability is quite low (25 millidarcy) resulting in an increased electricity demand of the pumps.

This wide range emphasizes the importance of conducting LCAs for deep geothermal heat plants to identify key parameters and reduction potentials. A case study of a hypothetical geothermal plant in Scotland shows similarly low results as the Rittershofen plant with 9.7 to 14.0 g CO_2 eq./kWh (McCay et al., 2019). The corresponding results are significantly influenced by the electricity mix, which for the Scottish plant is modeled according to the development of the UK mix with an average of 280 decreasing to <100 g CO_2 eq./kWh_{el} over the plant's lifetime. The Scottish plant, however, assumes a lower load factor of 60 % compared to 77 % for the Rittershofen plant, which is connected to a starch plant. The demand by the starch plant is mostly independent of seasonal heat demand changes in contrast to the residential demand of the Scottish study (Milligan et al., 2016). Besides the operational phase, the construction of the wells significantly influences the plants' environmental impact. Gkousis et al. (Gkousis et al., 2022) investigated a Belgian heat plant that resulted in 27 g CO_2-eq/kWh. The common aspect of relatively low results is, on the one hand, that peak load and redundancy were not taken into account and, on the other hand, that the electricity mix used has a relatively low GWP.

Since geothermal heat is suitable as baseload technology, peak load and redundancy coverage are usually necessary to ensure a secure supply of heat to consumers at all times. This is of particular importance to the operators. Neglecting those aspects in the LCA might lead to an underrepresentation of environmental impact, especially since it is often covered with fossil sources. The study by Pratiwi and Trutnevyte (Pratiwi and Trutnevyte, 2021) on medium-depth geothermal systems give a basic impression of the impact of implementing peak load. They demonstrate that increasing the share of supplementary heat for peak load from 10 to 50 % significantly increases the environmental impact from 31.64 to 95.45 g CO_2 eq./kWh (Pratiwi and Trutnevyte, 2021). Natural gas and waste incineration provided the supplementary heat in equal parts. The environmental impact is expected to increase significantly with a higher share of fossil heat.

In conclusion, deep geothermal sources for heating are significantly underrepresented in the literature compared to studies on power plants, especially based on real operational data. Additionally, most studies focus solely on geothermal energy, disregarding peak load and redundancy coverage usually achieved with fossil fuels and are necessary for covering the varying heat demand. This study takes a step towards filling these gaps by conducting LCAs for two currently operating geothermal heat plants. Thereby, analyzing seven impact categories most relevant for the geothermal sector (according to Parisi et al. (Parisi et al., 2020)) to give a holistic overview of the environmental burden including auxiliary energy demand. The plants are located in the Southern German Molasse Basin in the greater Munich area and vary mainly in the geothermal water temperature and, subsequently, auxiliary energy demand. To enhance the relevance and transferability of the findings, the two case studies were deliberately selected based on their distinct technical and operational characteristics, representing different boundary conditions within the same geological region. Additionally, the influence of auxiliary energy is investigated, and the potential for

[1] Cradle-to-gate approach and results from plant configuration with reinjection of geothermal fluid in a well, converted from original 52.15 kg CO_2 eq./GJ (Zhang et al., 2020).

Table 1
Overview of LCA studies on deep hydro-geothermal heating plants.

Location	Type of study	Well depth [m]	Peak load coverage	Electricity mix/ GWP [g CO_2 eq./kWh_{el}]	GWP [g CO_2 eq./kWh]	Reference
France, Rittershofen	Case study	2500	Not considered	French mix 2020[b]/ not specified	3.8	(Douziech et al., 2021)
China	Conceptual model	1400	Not considered	Coal power/ not specified	187.7	(Zhang et al., 2020)
Germany, Upper Rhine Valley	Planned	3500	Not considered	German mix 2025–2050/ 176.6	5.6	(Maar and Seifermann, 2023)
UK, Scotland	Conceptual model	1800–3000	Not considered	UK mix/280 - <100	9.7 - 14.0	(McCay et al., 2019)
Belgium	Case study + Conceptual model	3100, 4142	Not considered	Belgian mix 2020[a]/ not specified	11 –27	(Gkousis et al., 2022)
Northern Belgium	Case study	3957.2 and 4328	Not considered	Belgian mix 2020–2040/ not specified	58.5	(Gkousis et al., 2024)
Switzerland, State of Geneva	Conceptual model	3464	Natural gas and waste incineration	Hydropower/not specified	31.64 - 95.45	(Pratiwi and Trutnevyte, 2021; AS Pratiwi and Trutnevyte, 2021)

[a] : biggest shares: 47.8 % nuclear, 24.4 % natural gas (Gkousis et al., 2022).
[b] : biggest shares: 66 % nuclear, 11 % nuclear (Douziech et al., 2021).

reducing the environmental impact is analyzed through scenario analyses regarding electricity mix and potential fuels for peak load coverage.

2. Goal and scope

The LCA in this study is conducted according to ISO 14044 and 14040 (International Organization for Standardization, 2006; DIN Deutsches Institut für Normung e.V, 2021) including the four phases: definition of goal and scope, inventory analysis, impact assessment and interpretation. The following sections describe these phases in detail.

2.1. Objective

This study aims to conduct an LCA of two currently operating geothermal heating plants, including their district heating networks (DHN) located in the Southern German Molasse Basin. The plants mainly differ in geothermal water temperature but also plant configuration. To ensure comparability, boundary conditions suggested in (Parisi et al., 2020) are applied for this paper. Additionally, this study analyzes the use of auxiliary energy sources by conducting scenarios for the electricity mix and peak load coverage. The applied electricity mix is compared to the predicted energy mix in the year 2050 based on the location-based German electricity mix. For peak load coverage, the fuels evaluated include heating oil, natural gas, and biomethane.

For the LCA, energy and material flows are considered for the life cycle stages construction, operation and decommissioning (Fig. 1) using the LCA data base ecoinvent. Thus, a cradle-to-grave approach is applied. To ensure comparability with other LCAs, a lifetime of 30 a is chosen, as suggested by Parisi et al. (Parisi et al., 2020). According to Ortner et al. (Ortner et al., 2023) and Oliver-Solà et al. (Oliver-Solà et al., 2009), DHNs exceed the lifetime of the heat plant with respectively minimally 40 and 50 a. Therefore, it is assumed that the DHN will either be used by another heat plant immediately or remain unchanged in the ground until a new use. Either way, no decommissioning scenario is attributed to the geothermal plant's life cycle.

For operators of geothermal heating plants and decision-makers, these results may be helpful in developing strategies to reduce the environmental impact along with planning future plants.

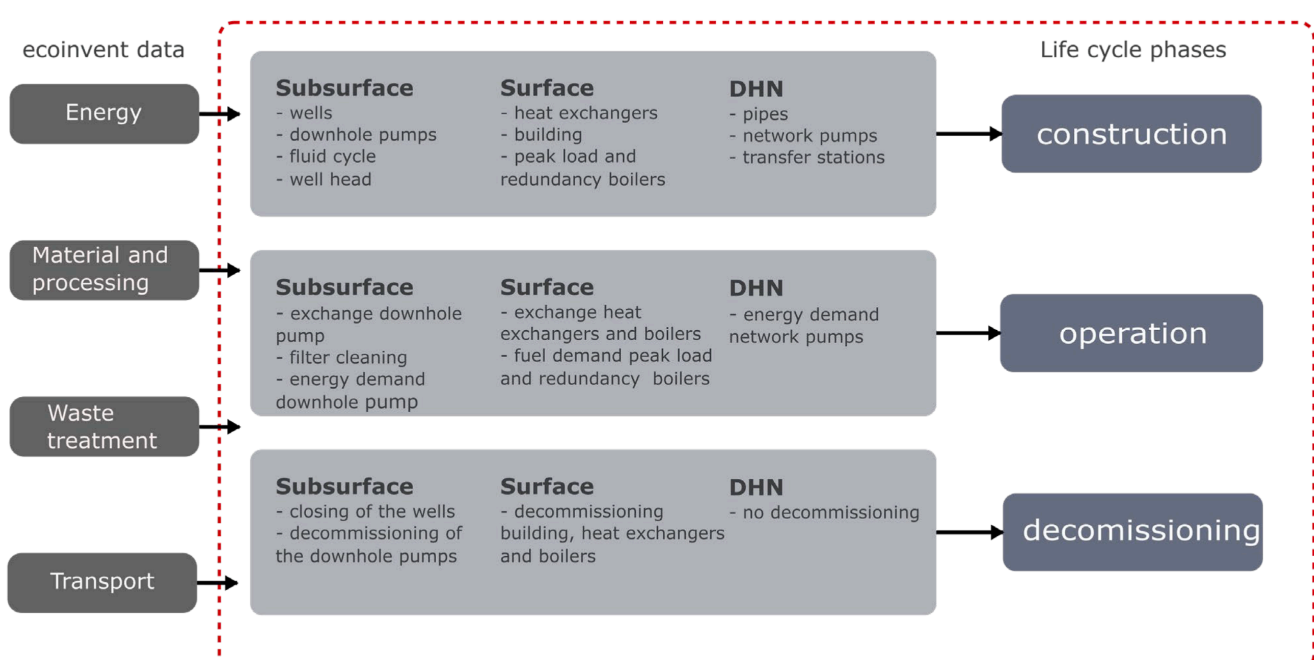

Fig. 1. LCA boundaries of the geothermal systems and their district heating networks (DHN).

2.2. Functional unit

In order to present the results in a comparable way, all energy and material flows are related to one variable, according to ISO 14044 (International Organization for Standardization, 2006). In this study, in line with Parisi et al. (Parisi et al., 2020), 1 kWh of net energy at the consumer has been selected for this purpose. This means that both DHN losses and the generation of additional energy to cover peak loads and provide redundancy by oil and gas boilers were considered.

2.3. System description and boundaries

In this section, the analysed geothermal plants as well as the considered electricity mix and peak load and redundancy scenarios are introduced.

2.3.1. Geothermal heating plants

The plant specifications are already listed in Table 2. Plant A was put into operation in 2005 and plant B in 2011. Both plants are located in the Southern German Molasse Basin, characterized by a porous, water-bearing carbonate rock layer situ at a depth of 2000 to 3000 m in the greater Munich area (Keim et al., 2020). As the depth increases, the temperature of the geothermal water rises naturally. This explains why plant A, situated south of Munich, exhibits higher temperatures exceeding 103 °C with almost double the length of the production wells when compared to plant B, located to the north, which has production temperatures of only 73 °C. During the operation of the plants, it is assumed that the temperatures of the thermal water will remain constant and that there will be no thermal breakthroughs. This aligns with the findings of Fadel et al., who observed a thermal breakthrough in only one of thirteen plants in the Molasse Basin (Fadel et al., 2022).

Additionally, plant A has two production wells, whereas plant B only has one. The hot geothermal water is coupled by heat exchangers to the DHN fed back into the injection wells. Additionally, boilers are installed to cover peak load and redundancy in case of maintenance or component failure. Since plant B's extracted geothermal water temperature is relatively low, a significant amount of auxiliary energy supplied by the boilers is needed to reach the average DHN supply temperature of around 80 °C and to increase total thermal power output. As fuel for the boilers plant A uses heating oil as does plant B for the first two years, afterwards only natural gas is used. Three years after plant B went into operation, a gas-fuelled cogeneration unit (CU) was installed that primarily generates electricity but also supplies additional thermal energy to the DHN. Fig. 2 shows a schematic depiction of the plants. Residual electricity demand that cannot be met with the CU is provided by the German grid, as is the total demand of plant A. Thereby the specific electricity mix of each year is considered (see Section 2.3.3).

The operation data regarding heat output and auxiliary energy demand is based on real measured data provided by the plant operators. The heat demand is not constant throughout the system's life time, but increases gradually after commissioning as consumers are connected gradually as depicted in Fig. 3. For plant A (dark grey) and plant B (red) actual measured data (open symbols) is used as well as projections to estimate future and previous developments (filled symbols) based on information provided by the operators.

For the first three to seven years a linear increase was estimated including a plateau phase for plant A that added another production well in year seven to increase heat output. The future demand development is projected using actual data on annual energy consumption and production. It is assumed that there will be a linear increase, consistent with the increases of previous years. Furthermore, a yearly decrease of the heat demand of 0.7 %, as stated in Kemmler et al. (Kemmler et al., 2020) as a "continue as before" reference scenario, is considered. The decrease is due to an expected increase in insulation standards and milder winters. Both the peak load demand and the electricity demand are based on measured data, and the relationship between electricity and fuel demand and total annual heat output is assumed to remain constant in the future as it has been in previous years with measured data.

To clarify the operational strategy of the systems, measured annual load duration curves from two representative geothermal plants were included. Fig. 4 presents the sorted thermal load profiles of Plant A (2015) and Plant B (2019). These data reflect real operating behaviour over a full year and provide a realistic impression of capacity utilization, partial-load operation, and demand variations.

The main difference is evident in the proportion of peak load and redundancy boilers, which is significantly higher for plant B. The additional base load provided by the cogeneration unit is also visible.

In Table 2 the average energy demand and heat output are listed. Regarding DHN, plant A has almost double the length of plant B's with 48.5 to 21.2 km. This is due to the higher number of buildings with lower heat demand that are also more dispersed in plant A's case.

Table 2
Specifications of the investigated geothermal heat plants, plant A partly based on (Uhrmann et al., 2023).

Parameter	unit	Plant A Value	Plant B
Commissioning year	a	2005	2011
Installed power – geothermal	MW	16.7	8.2
Installed power – peak load and redundancy boilers	MW	17.0	21.8
Cogeneration unit[a]		–	
Electric	MW_{el}		0.55
Thermal	MW		0.59
Average yearly net heat output	MWh/a	55 497	46 876
Average yearly oil consumption-boiler	MWh/a	2 982	102[b]
Average yearly gas consumption-boiler	MWh/a	–	22 367[b]
Average yearly gas consumption-cogeneration unit	MWh/a	–	9 237
Average yearly electricity coverage from the grid	MWh/a	5 519	711
Production well 1 measured depth	m	4 666	2 450
Production well 1 brine temperature	°C	107	73
Production well 1 flow rate	kg/s	55	100
Production well 2 measured depth	m	4 120	–
Production well 2 brine temperature	°C	103	
Production well 2 flow rate	kg/s	26	
Injection well measured depth	m	3 984	2 166
Injection brine temperature	°C	66	no data
DHN			
DHN total length	km	48.5	21.2
DHN connectors	–	965	160

[a] : The cogeneration unit went into operation in the fourth year of operation plant B.
[b] : The boilers were operated with heating oil the first two years.

2.3.2. Peak load and redundancy

In the respective base case plant A utilizes heating oil in boilers for peak load and redundancy coverage whereas plant B only uses heating oil in the first two years. Afterwards, natural gas from the grid is used. The CU also obtains natural gas from the grid. To compare the conventional fuels, heating oil and natural gas, respective scenarios are created for each plant. Additionally, consideration is given to the renewable fuel source of biomethane, which is derived by upgrading biogas through chemical means, increasing its methane content to match that of natural gas (Lauf et al., 2023).

For the use of biomethane two scenarios are created, one with the sole use of biomethane as fuel and the second with a mixture of biomethane and natural gas. The latter is created as an optimistic but realistic approach since the production volume of biomethane in Germany is limited. This is due to the restrained availability of the biogas feedstock agricultural and animal waste as well as energy plants. The latter are in competition for cultivable land for food or feed crops as well

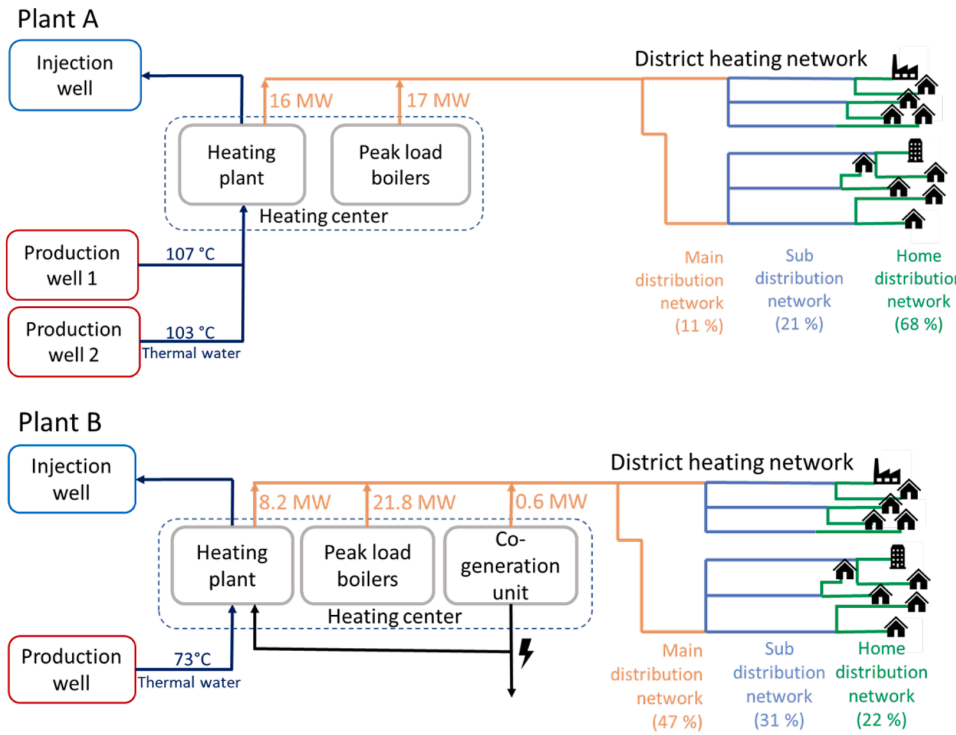

Fig. 2. Schematic representation of the plant configurations of plant A and B.

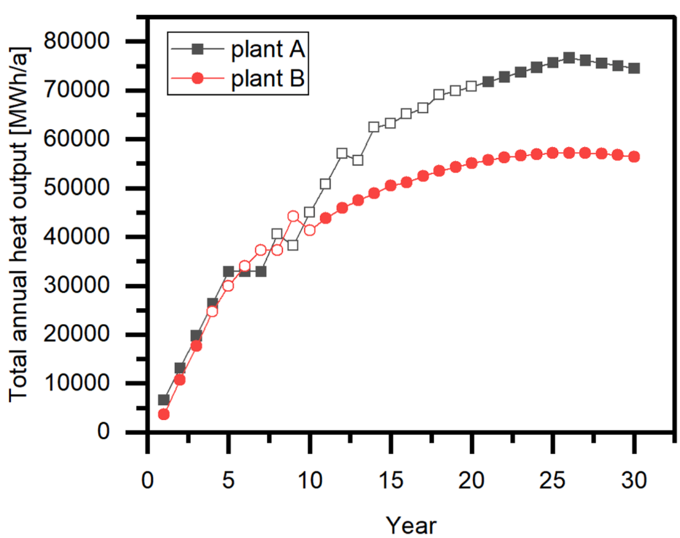

Fig. 3. Total annual heat output of plants A and B over their operational lifetime. Open symbols represent actual measured data, while preceding and projected values are based on expansion plans and information provided by the operators as well as projections of the change in heat demand based on (Kemmler et al., 2020).

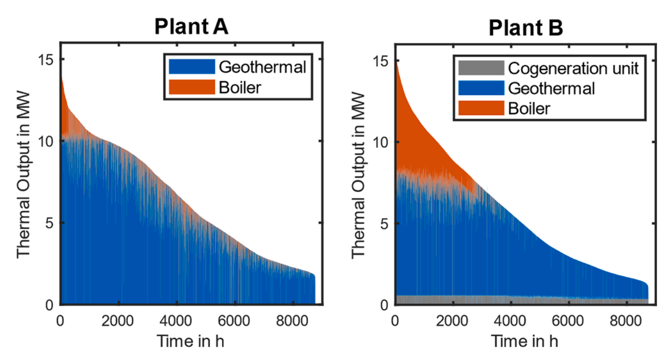

Fig. 4. Sorted thermal load profile of plant A (2015) right and plant B (2019) left.

as the use of biogas for electricity production (7.8 % of the electricity mix in 2022 (Federal Network Agency Germany, 2023)) (Lauf et al., 2023; Bettgenhäuser et al., 2023). The European REPowerEU Plan of May 2022 includes scaling up biomethane until 2030 to 366 TWh (original 35 billion cubic meters (bcm) with 1 bcm = 10.467 TWh) (European Commission, 2022). The potential for Germany in 2030 is estimated with 82.6 TWh by Alberici et al. (Alberici et al., 2022). Assuming a similar natural gas consumption than for 2021 with 908 TWh (Eurostat, 2023), 9 % of natural gas can be substituted with biomethane in 2030 (for the sake of simplicity, it is assumed that 100 % of the biomethane is fed into the gas grid). Assuming a reduction of the total gas demand due to switching to renewable sources, for the realistic scenario the value of 10 % biomethane in the natural gas grid is chosen. This biomethane share is also already currently commercially offered in the state of Baden-Württemberg in Germany (Pehnt et al., 2018). Table 4 gives an overview over the different scenarios that are analysed for each plant.

Since the peak load scenarios include the assumption that biomethane is supplied by the natural gas grid, the fuel supply for the CU naturally also is affected by the gas mix of the grid and therefore receives the same supply in the described scenarios Biomethane and 90NG 10 BM.

For the LCI plant components necessary for using light fuel oil, like the oil storage and catch basin are no longer needed and are therefore excluded. Through the ecoinvent data the gas production and the natural gas grid is considered proportionally. The material and energy input for the boilers are assumed to be the same for the fuel oil and gas, analogous to Faist-Emmenegger et al. (Eurostat, 2007). Since biomethane is used to substitute natural gas, the same infrastructure as for

Table 4
Parameters for the peak load scenarios with the base case (heating oil), natural gas and biomethane (Uhrmann et al., 2023).

Parameter	Heating oil	Natural gas	Biomethane
Annual efficiency	91 %[a]	96 %[b]	96 %[c]
Plant components	Boiler Chimney	Boiler[d] Chimney	Boiler[d] Chimney
Fuel supply	Oil storage and catch basin	Natural gas network	Natural gas network
Direct emissions per kg light fuel oil/ m^3 high pressure gas according to ecoinvent process	Heat production, light fuel oil, at industrial furnace 1MW	Heat production, natural gas, at boiler modulating >100kW	Heat production, natural gas, at boiler modulating >100kW[e]

[a] : Annual efficiency for the year 2019 at plant A, assumed to remain the same for plant B and to be constant over their life times.
[b] : For a modulating, not condensing boiler according to (Eurostat, 2007).
[c] : Same value assumed as for natural gas.
[d] : The same inputs are considered as for the oil fuelled boiler analogous to (Eurostat, 2007).
[e] : All emitted greenhouse gases are biogenic and are therefore not relevant for the GWP.

natural gas (gas network and boilers) is assumed as well as the same emissions for the burning in the boilers. The greenhouse gas emissions for the burning of biomethane, however, are considered as biogenic and are therefore not part of the CC-impact. The extensive LCI with the selected ecoinvent data for the components and the process of burning of the fuels can be found in the appendix in Table A.4. An overview of the relevant parameters and considered infrastructure for the respective scenarios is shown in Table 4. For the scenario with 10 % biomethane and 90 % natural gas the models for natural gas and biomethane from Table 4 are considered proportionally.

For plant B additional to every peak load scenario there is one scenario added without the CU (nCU). Thereby the electricity demand is covered by the grid and the heat output from the CU is substituted with the peak load boilers. The boilers are chosen instead of geothermal energy since it is assumed that heating from the CU is used to increase the supply temperature for the DHN network, which is necessary since the thermal water temperature is lower than the DHN supply temperature. Table 3 provides an overview of the scenarios.

2.3.3. Electricity mix

To analyse the ecological potential of changing the consumed electricity mix to a more renewable one, the base case is compared to the German electricity mix in 2050 applying the “start scenario” by Fattler et al. (Fattler et al., 2019).

The base case includes the location-based electricity mix in Germany for the respective electricity demand for each year over the plants’ lifetime of 2005–2035 for plant A and 2011–2041 for plant B. The data for past years is obtained from the Federal Network Agency Germany (Federal Network Agency Germany, 2023) and the future German electricity mix is obtained from the projection of Flattler et al. (Fattler et al., 2019) again applying the “start scenario”. The average shares of power sources can be found in Table 5. Analog to Section 3.2, the results for electricity mix scenarios that are shown in this section are reduced to the impact categories ACI, CC and RUf. All results for the residual impact categories as well as numerical values are listed in the appendix in Table A.3.

Table 3
Peak load scenarios for plant A and B and considered fuels.

Scenario	Base case	Heating oil	Natural gas	Biomethane	90NG 10BM
Plant A	Heating oil	/	Natural gas	Biomethane	90 % natural gas 10 % biomethane
Plant B					
Peak load and redundancy boilers	0.5 % heating oil 99.5 % natural gas	Heating oil	Natural gas	Biomethane	90 % natural gas 10 % biomethane
CU	Natural gas	Natural gas	Natural gas	Biomethane	90 % natural gas 10 % biomethane

2.4. Data source and methodology

In this section, the topic of data quality is addressed which needs to be included in any report for a LCA according to ISO 14,044 (International Organization for Standardization, 2006). For this study, primary data from the plant operator was utilized whenever possible. If such data was unavailable, relevant literature was considered. Thereby, it was ensured that the applicability was given, e.g. through suitable geographical and time related similarity. The data sources are detailed in the LCI (see Table 7).

To perform the LCA, SimaPro software (version 9.5.0.0) and the ecoinvent database (version 3.9.1) were used. Within ecoinvent, the “allocation cut-off by classification system” model was selected. Ecoinvent provides the characterization factors for the allocation of environmental impacts to perform the Life Cycle Impact Assessment (LCIA), which considers, for example, how much greenhouse gas is emitted for each energy and material input and output collected in the Life Cycle Inventory (LCI) phase.

Environmental impacts for the respective impact categories (I_{cat}) were calculated by multiplying LCI data (A_i), such as material and energy inputs, with category-specific impact factors (EF_i) derived from the ecoinvent database:

$$I_{cat} = \sum_i (A_i \cdot EF_i) \tag{1}$$

The results were aggregated for each life cycle phase and normalized to the functional unit of 1 kWh of the total net heat output over the life time Q:

Table 5
Composition of the examined electricity mixes and their respective environmental footprint. For plant A the base case displays the general German electricity mix for the years 2005–2035 (extension to (Uhrmann et al., 2023)) and 2011–2041 plant B considering the differing yearly energy demands of the heat plants over the life time. The years 2005–2021 are modelled after (Federal Network Agency Germany 2023). Future mixes are modelled according to (Fattler et al., 2019) (start scenario). 2050 displays the market based energy mix in the year 2050 according to (Fattler et al., 2019).

Energy source	Share [%]		
	Plant A 2005–2035	Plant B 2011–2041	2050
Natural gas	15.9	16.9	17.6
Nuclear	10.2	5.5	0.0
Lignite	16.2	9.7	0.0
Hard coal	12.4	7.4	0.0
Biomass	8.4	9.2	7.3
Hydro	3.6	3.8	3.2
Wind offshore	6.4	11.4	22.6
Wind onshore	17.4	23.6	33.0
Solar	7.8	10.4	13.7
Geothermal	0.6	0.8	0.8
Pump storage	1.1	1.2	1.3
Lithium-ion battery	0.0	0.1	0.5
Environmental footprint			
ACI [mmol H^+ eq./kWh_{el}]	1.306	1.082	0.685
CC [g CO_2 eq./kWh_{el}]	494.1	369.0	170.1
RUf [MJ/kWh_{el}]	6.646	4.861	2.280

$$I_{cat,FU} = \frac{I_{cat}}{Q} \quad (2)$$

For the results as recommended in (Parisi et al., 2020), the European Commission's Environmental Footprint (EF) method was selected, but instead of the version 3.0 (Fazio et al., 2018), the in 2022 updated version 3.1 (Andreasi Bassi et al., 2023) was used. Parisi et al. (Parisi et al., 2020) categorized the impact categories into levels of relevance for the geothermal sector. In this work, all categories classified as "high relevance" are considered and listed in Table 6 including the level of relevance from (Fazio et al., 2018).

3. Results and discussion

3.1. Base case

3.1.1. LCI of the base case

The base case for both plants includes the construction on the subsurface level with wells, the geothermal fluid circuit, wellheads, and well pumps. For the heating center, this contains the heat exchangers, peak load and redundancy boilers, and main plant components. In addition, the DHN is considered according to its length (stated in Table 2). For the operation phase, energy consumption for peak load and redundancy as well as electricity consumption and maintenance are included as detailed in Table 2. The composition of the electricity mix is discussed in detail in Section 3.3. Finally, the end-of-life phase covers the disposal of the heating plant components and the closure of the wells. The detailed LCIs can be found in Table 7, including the complete LCI of plant A, which is an updated version of the LCIs in (Uhrmann et al., 2023) and (Uhrmann et al., 2022).

As this is a cradle-to-grave assessment, the upstream supply chains for material production—including raw material extraction and refining—are fully captured through background data from the ecoinvent 3.9.1 database. This includes processes such as metal ore mining, mineral processing, and energy-intensive refining steps for materials like copper, steel, aluminium, and bitumen, which are used in components such as heat exchangers, pipelines, insulation systems, and DHN infrastructure. The subsequent processing of these raw materials into final components, such as pipes or structural parts, is also included via the corresponding background datasets.

Table 6
Considered midpoint impact categories with high relevance for the geothermal sector as recommended by (Parisi et al., 2020) based on (Fazio et al., 2018).

Characterization factor	Indicator	Unit	Level of recommend-dation[a]
Climate change (100a)	Radiative forcing as Global Warming Potential (GWP100)	kg CO2 eq.	I
Human toxicity, cancer effects	Comparative Toxic Unit for Human Health (CTUh)	CTUh	III
Human toxicity, non cancer effects	CTUh	CTUh	III
Ecotoxicity freshwater	Comparative Toxic Unit for ecosystems (CTUe)	CTUe	III
Acidification	Accumulated Exceedance (AE)	mol $H+$ eq.	II
Resource depletion – Minerals and metals	Abiotic Depletion Potential (ADP) ultimate reserves	kg Sb eq.	III
Resource depletion – Energy carriers	ADP fossil	MJ	III

[a] : according to International Life Cycle Data system levels: recommended and satisfactory-Level I, recommended but in need of some improvements – Level II or recommended, but to be applied with caution – Level III (Fazio et al., 2018).

3.1.2. LCA of the base case

For a general overview the overall results for plant A and B are listed Table 8 for the selected impact categories:

To further analyze the contributions of the life cycle phases and compare them between the two plants, relative results are presented in Fig. 5. The interpretation of the results is structured according to the contribution of each life cycle stage and key infrastructure component. The single impacts of the plants are compared relative to the plant with the highest overall impact. The results are normalized to the higher absolute value of the plants. The shares for the plants' components, however, are relative to the total impact of each plant.

A detailed breakdown of the results of the construction phase can be found in the Appendix in Table A.6-A.11 for the two plants.

3.1.2.1. Acidification (ACI). The operational phase is the biggest contributor to the ACI category since it releases emissions from combustion-based energy generation: such as coal power plants for the consumed German electricity mix and combustion of heating oil and natural gas for peak load and redundancy coverage. These emissions are particularly significant because NH_3, NO_2, and SO_X air pollutants are the main cause of ACI (Fazio et al., 2018). Additionally, construction processes that rely on auxiliary energy produced by diesel burned in a generation set for drilling wells or installing the DHN also contribute to ACI. For the later the production of fossil material bitumen that is used to replace the asphalt for installation under streets has a significant contribution to the ACI. When compared, plant B has a slightly lower (by 14 %) impact than plant A.

Since the German electricity mix has a significant share of coal-based sources (32.8 % in 2022 (Federal Network Agency Germany, 2023)) but is gradually increasing its usage of renewable energy sources, the difference between the older plant A and newer plant B can be attributed to the former's higher reliance on coal-based electrical power. Additionally, Plant B sources a significant amount of its electricity demand from the CU rather than the German grid.

3.1.2.2. Climate change (CC). Especially CC impact is influenced by the operation phase. The high fossil resource consumption of plant B in particular is reflected negatively here. Thereby, plant A emits significantly less with only 42 % of plant B's impact. However, the German electricity mix over plant A's lifetime over the years 2005–2035 (used mainly for the downhole and network pumps) still has significant fossil shares with over 50 %, which in turn appears as the biggest single impact. Based on the EU taxonomy threshold of 100 g CO_2 eq./kWh (EU Technical Expert Group on Sustainable Finance, 2020), plant A is suitable as a renewable source in accordance with the 1.5 °C global warming constraint. Conversely, plant B with the commissioning year 2011 surpasses the threshold with almost double the impact. This makes the need for improvement strategies, addressed later in this study (see chapter 3.2 and 3.3), apparent and additionally underlines the importance of conducting LCAs for geothermal heating.

3.1.2.3. Freshwater ecotoxicity (FET). FET impact is dominated by the construction phase. Especially the construction of the DHN has a big impact due to the petroleum product bitumen. Petroleum and natural gas extraction produce water discharge that has a high impact on FET (0.19 CTUe/kg), which is the most significant single impact in this category. Per kg bitumen thereby 5 g of wastewater is discharged from petroleum extraction. Furthermore, the production of polyurethane foam used for the insulation of the DHN-pipes have additional impact because of the use of the organic compounds aniline and polyols for its production. Other aspects include the release of potassium carbonate for drilling mud explaining the greater impact of the subsurface construction on this impact category.

For the operation phase, the fossil shares of the electricity mix especially lignite due to mine operation increase the FET impact. But

Table 7
Complete LCI of plant A and B (updated version for plant A in (Uhrmann et al., 2023) and (Uhrmann et al., 2022).

Parameter	Description	Unit	Value		Source
			Plant A	Plant B	
Construction					
subsurface					
Drilling site preparation	Cement, unspecified	kg/well	300	300	(Frick et al., 2010)
	Diesel, burned in building machine	MJ/well	20,000	20,000	(Frick et al., 2010)
Drilling rig drive	Diesel in construction equipment	GJ	12,431	11,447	Operator
Geothermal fluid cycle	DHN pipes DN250 installed in urban area	m	4300	1980	Operator, (Menberg et al., 2023)
Deep well pump	Steel, low-alloyed and metal working	kg	1224	400	Operator, (Rogge, 2003)
	Steel, chromium steel 18/8 and metal working	kg	10,927	3570	Operator, (Rogge, 2003)
	Aluminium bronze and metal working	kg	2449	800	Operator, (Rogge, 2003)
	Transport, freight, lorry 16–32 t, euro3	tkm	9490	3101	Operator
Well casing	Steel, chromium steel and drawing of pipes	t	328	109	Operator
	Steel, low-alloyed and drawing of pipes	t	667	219	Operator
Well cementation	Cement, Portland	t	964	9	Operator
	Cement, CEM III/A	t	–	287	Operator
	Chemical, inorganic	kg	6144	1846	(Frick et al., 2010)
	Water, decarbonised	kg	259,584	130	(Frick et al., 2010)
Reservoir enhancement	Water, deionised	t	775	301	Operator
	Diesel, burned in diesel-electric generating set	GJ	10	5	(Frick et al., 2010)
	Hydrochloric acid	t	130	129	Operator
Drilling mud	Diesel, burned in diesel-electric generating set	GJ	2315	837	(Frick et al., 2010)
	Drilling waste	t	5151	2300	Operator
	Waste cement	t	431	200	Operator
	Waste water	t	218	–	Operator
	Drilling fluid	T	2513	820	Drilling company
Transport subsurface	Transport, freight, lorry >32 t	tkm	432,000	288,000	(Frick et al., 2010)
	Transport, freight train	tkm	1239,000	826,000	(Frick et al., 2010)
surface					
3 heat exchangers	Steel, chromium steel and metal working	kg	13,010	6553	Operator
	Titanium, primary	kg	1169	1169	Operator
peak load and redundancy boilers[a]	Crude oil/natural gas boiler	–	3	4	Comparable data
Oil storage and catch basin[a]		–	1	0.25	Comparable data
Chimney[a]		–	1	1	
Cogeneration unit	Steel, low-alloyed and metal working	t	–	6	operator
	Transport, freight, lorry >32 t	tkm	–	308	(Eurostat, 2007)
	Transport, freight train	tkm	–	3696	(Eurostat, 2007)
Building	Steel, low alloyed	t	86	86	Operator PB
	Concrete block	m^3	1668,394	1668,394	Operator PB
	Diesel, burned in building machine	MJ	1000	1000	Operator PB
DHN[e]	Plastic sheath pipes, connectors, trench work, transport, transfer stations, network pumps	km	48.5	21.5	Operator, (Menberg et al., 2023; Biemann, 2015)
Operation[b]					
Disposal filter residues and scaling	Transport, freight, lorry >32 t	tkm	15,000	15,000	(Frick et al., 2010)
	Disposal of hazardous waste	kg	12,749	12,749	(Frick et al., 2010)

(*continued on next page*)

Table 7 (*continued*)

Parameter	Description	Unit	Value		Source
			Plant A	Plant B	
Exchange of downhole pump	Steel, chromium steel	t	51.10	51.10	(Frick et al., 2010; Rogge, 2003)
	Scrap steel	t	51.10	51.10	(Frick et al., 2010; Rogge, 2003)
	Transport, freight, lorry >32 t	tkm	3500	3500	(Rogge, 2003)
Exchange of heat exchanger plates	Scrap steel	kg	2426.09	2426.09	Operator PA
	Steel, chromium steel	kg	2426.09	2426.09	Operator PA
	Titanium, primary	kg	1169.07	1169.07	Operator PA
Decommissioning					
Closing of the wells	Gravel, crushed	kg/m well	51.10	51.10	(Frick et al., 2010)
	Cement, unspecified	kg/m well	4.90	4.90	(Frick et al., 2010)
Dismantling surface	Scrap steel	t	173[c]	198[d]	

[a] : detailed LCI in Table A.4.
[b] : without auxiliary energy consumption (electricity and fuels) which is detailed in Table 2 and Table 5.
[c] : including steel for heat exchangers and boiler – decommissioning of the oil storage and chimney is already considered.
[d] : including steel for heat exchanger, cogeneration unit, and boilers – decommissioning of the oil storage and chimney is already considered in the process.
[e] : detailed LCI in Table A.5.

also, other aspects affect the FET impact of the electricity mix negatively like the sodium hydrochloride consumption in nuclear power plants used to counteract biofouling in cooling water. Therefore, plant A has a 29 % higher impact than plant B.

3.1.2.4. Human toxicity, cancer (HTC). This category out of all is influenced most by the construction phase. Especially because of steel that is used in the DHN, the well's casing and the surface components. The significant impact of steel production results from using coke in the production process and treating electric arc furnace slag. For plant B, the steel used for the natural gas distribution network additionally contributes to HTC in the operation phase. Another aspect is the insulation material polyurethane foam for DHN pipes. Combined with plant B's higher steel input, its impact surpasses that of plant A.

3.1.2.5. Human toxicity, non-cancer (HTNC). This category again is dominated by the operation phase. Affecting mainly plant A, electricity consumption has a high HTNC impact due to the copper used for the infrastructure and grid. The natural gas consumption of plant B also has a significant impact due to emission from burning waste gas and vented gas from gas production. The construction phase is mainly influenced by steel demand for the wells as well as drilling waste on the subsurface side but also by polyurethane for the DHN pipe insulation and bitumen for installation under streets. Again, the electricity consumption from the German grid determines the higher impact of plant A compared to plant B.

3.1.2.6. Resource use, fossil (RUf). Since this category relies on fossil fuels, it is expected that the operation phase utilizing gas and oil for peak load and redundancy as well as electricity generation for plant B accounts for the majority of the impact. Furthermore, due to plant B's significantly higher consumption, plant A's RUf is 65 % lower.

3.1.2.7. Resource use, minerals and metals (RUm). The RUm impact is mainly based on the consumption of copper that is used for the electricity distribution network. Another aspect affecting the electricity mix is the silver that's used for solar power plants. The amount of steel used in the construction phase also has a significant impact due to the chromium for high alloyed steel. The impact of the peak load for plant B is due to the usage of copper for the natural gas distribution infrastructure. Since the electricity mix has a higher impact on plant A that obtains electricity solely from the grid, for RUm plant A has a 55 % higher impact than plant B.

Comparing both plants, it is apparent that the main differences stem from the operational phase. Interestingly, there is not one plant that is superior in all or even most categories, but they differ significantly from category to category. Plant A performs better in the categories CC, HTC and RUf and plant B in ACI, FET, HTNC and RUm.

In order to put the results into perspective and support their plausibility, they are discussed and evaluated in comparison with existing LCA studies on geothermal plants with comparable configurations and boundary conditions, as listed in Table 1. Plant A most resembles the geothermal plant with the configuration of medium-large depth in the generic study of Pratiwi et al. (Pratiwi and Trutnevyte, 2021). Thereby, the boundary conditions are similar with geothermal water temperatures of 105 °C, measured well depth of 3464 m and 10 % supplementary heat (although for this plant 5 % is allocated for cooling purposes). The hypothetical Genevan plant, however, covers electricity demand with 100 % renewable energy and therefore reaches the much lower value of 31.64 g CO2 eq./kWh compared to plant A's 81.37 g CO2 eq./kWh, which uses an electricity mix with a significant fossil share of 44.5 % (see Table 5). Additionally, the Genevan plant utilizes a mix of natural gas and waste incineration heat for peak load instead of plant A's heating oil based peak load and redundancy coverage. To quantify the reduction potential of a renewable electricity mix and peak load

Table 8
Environmental impacts of the base case scenarios of plant A and B.

Impact category	Unit per kWh	Plant A	Plan B
Acidification	mmol $H+$ eq	0.243	0.210
Climate change	g CO_2 eq.	81.372	195.182
Ecotoxicity freshwater	CTUe	0.531	0.412
Human toxicity, cancer	10^{-11}•CTUh	6.227	7.195
Human toxicity, non-cancer	10^{-10}•CTUh	8.630	5.703
Resource depletion – energy carriers	MJ	1.308	3.113
Resource depletion – minerals and metals	mg Sb eq.	0.497	0.275

coverage, corresponding scenario analyses are investigated in Sections 3.2 and 3.3. Looking at the analyzed impact categories of (Pratiwi and Trutnevyte, 2021), unfortunately, CC is the only common category out of the eight, since they chose different methods with ReCiPe 2016 and Cumulative Energy Demand.

Plant B is similar to the hypothetical Scottish plant (McCay et al., 2019), with a temperature range of 65 to 85 °C and a depth of 2000 to 2500 m regarding the geological boundary conditions. However, the impacts of plant B are significantly higher, by a factor of >10. This is primarily due to Plant B taking into account peak load and redundancy coverage, resulting in a significant consumption of natural gas, as well as electricity demand covered by natural gas-fueled CU. The emissions of the electricity mix are significantly lower, with an average of 190 g CO_2 eq/kWh$_{el}$ compared to the 369 g CO_2 eq/kWh$_{el}$ used for plant B (see Table 5). Additionally, the LCI of the Scottish plant does not include components for the heating center or maintenance work and the DHN. Therefore, the electricity demand is limited to downhole pumps. This study only considered CC, therefore other impacts can not be compared.

In summary, analyzing the life cycle phases, the end-of-life phase has a negligible impact. With the exception of FET and HTC, the environmental impact largely stems from the operational phase, which depends heavily on the consumption of auxiliary energy for peak load and redundancy coverage, as well as electricity usage. For this reason, the auxiliary energy coverage is examined further with scenario analyses in the following sections.

3.2. Peak load scenarios

In this sections fuel based peak load and redundancy technologies are compared for both plant A and B. Thereby, heating oil, natural gas and biomethane are considered for plant A and B. For Plant B, an additional scenario is included for each peak load case, where the scenario excludes the CU (referred to as nCU). In this scenario, the electricity demand is met by the grid, and the heat normally provided by the CU is instead supplied by the peak load boilers. The detailed model description can be found in Section 2.3.

For the sake of a clearer overview, only three impact categories are shown in the results. The selection was made here firstly according to the level of recommendation (Fazio et al., 2018) (see Table 6) and thus the categories CC and ACI were selected. RU fossil was selected as the third category because, on the one hand, it is associated with the EU's efforts to be more independent of fossil fuels (as seen in the RePowerEU Plan (European Commission, 2022)) and, on the other hand, when applying the normalization method of EF 3.1 (Andreasi Bassi et al., 2023), it is one of the categories with the highest score alongside CC and thus indicates higher relevance. The results of all categories from Table 6 and all numerical results can be found in Table A.1 and 2.

In Fig. 6 the LCA results for the peak load coverage are shown considering the different scenarios for ACI, CC and RUf. Next to the base cases, the scenarios include the coverage by heating oil (HO), natural gas (NG), biomethane (BM) and the realistic scenario with 90 % natural gas and 10 % biomethane (90NG10BM). For plant B the results with and without CU are depicted for each scenario.

All categories that utilize heating oil as their main fuel exhibit the largest impacts regardless of the category. Generally, all gaseous fuels lead to a reduction of the environmental impact. As expected, the greatest reductions in all categories are achieved with the use of biomethane. Even though the BM scenario is only slightly (2 %) better for ACI, because of the emissions (NH_4, N_2O) for the anaerobic digestion of manure for biomethane production. In general, the environmental performance of plant B is more affected by changes in fuel due to the higher consumption of fuels compared to plant A (see Table 2). Plant A exhibits the most significant reduction with the scenario BM in the category CC, achieving a notable reduction of 21 % compared to the base case. The effects are still much less drastic since the energy demand for peak load and redundancy coverage is significantly smaller than those of plant B (22 GWh/a natural gas compared to 3 GWh/a heating oil for plant A, see Table 2). The results for operating plant B with and without the CU differ greatly. For RUf and CC, the difference between operating with (CU) and without the cogeneration unit (nCU) is quite small. It shows a small reduction with nCU except for the impact categories HO and BM. Here the impact for the nCU scenario is higher than the CU scenario. Looking at the HO-scenario nCU is slightly higher. This can be explained with the substitution of the heating output of the CU unit by the peak load boiler. Heating oil has a much higher impact than heat generation with natural gas in the CU. In case of the BM-scenario, the nCU scenario is higher because the electricity generation in Germany has a greater impact than

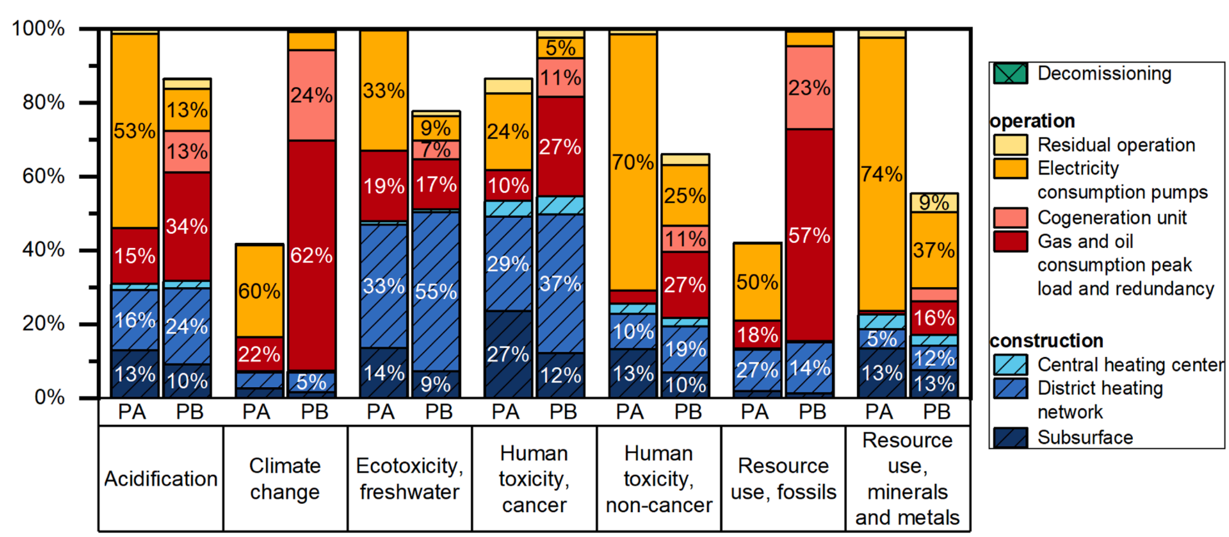

Fig. 5. Normalised LCA results of the geothermal heat plants A (PA) and B (PB) considering the life cycle phases construction, operation and decommissioning.

the CU electricity generation based on Biomethane. This is due to the higher proportion of fossil shares in the German mix. For ACI, nCU has a bigger impact for all scenarios. This is due to the high impact of the German electricity mix (see Section 3.1 on ACI) which is used to replace electricity coverage by the CU.

Since RUf is based on the caloric value of the fossil fuels, the difference between oil and natural gas is mainly due to the degree of utilization assumed for the use of natural gas (see Table 4). Plant B is only able to reduce CC impact to fit the taxonomy threshold of 100 g CO_2 eq./kWh (EU Technical Expert Group on Sustainable Finance, 2020) by switching to BM with 44.65 g CO_2 eq./kWh. With the realistic scenario, 90NG10BM for plant B nCU 181.22 g CO_2 eq./kWh can be achieved. By using biomethane, plant B would be in the GWP size range of the Belgian plant assessed by Gkousis et al. (Gkousis et al., 2022) (11–27 g CO_2 eq./kWh) and the conceptual model for a plant in Switzerland by Pratiwi and Trutnevyte (AS Pratiwi and Trutnevyte, 2021) (31–95 g CO_2 eq./kWh), which, however, have higher drilling depths.

To conclude, switching to natural gas from heating oil leads to a minor improvement. The biggest impact can be achieved with biomethane. Replacing the CU of plant B has, at best, a small positive effect, but can also have negative effects due to the replacement of heat generation with the boilers or the still high impact of the German grid, which is now solely covering the electricity demand. An increase of biomethane in the gas pipelines significantly decreases the environmental footprint of the plants. However, it has to be considered that the biomethane share in the gas network is dependent on the development of the gas market. Especially considering the potential for future biomethane production, it has the capability to more than double in Germany by 2050 (Alberici et al., 2022) as there is great potential for expanding biomethane produced by thermal gasification in contrast to anaerobic digestion (Alberici et al., 2022). Other gas based fuel sources could become relevant in the future as well, for example Wachsmuth

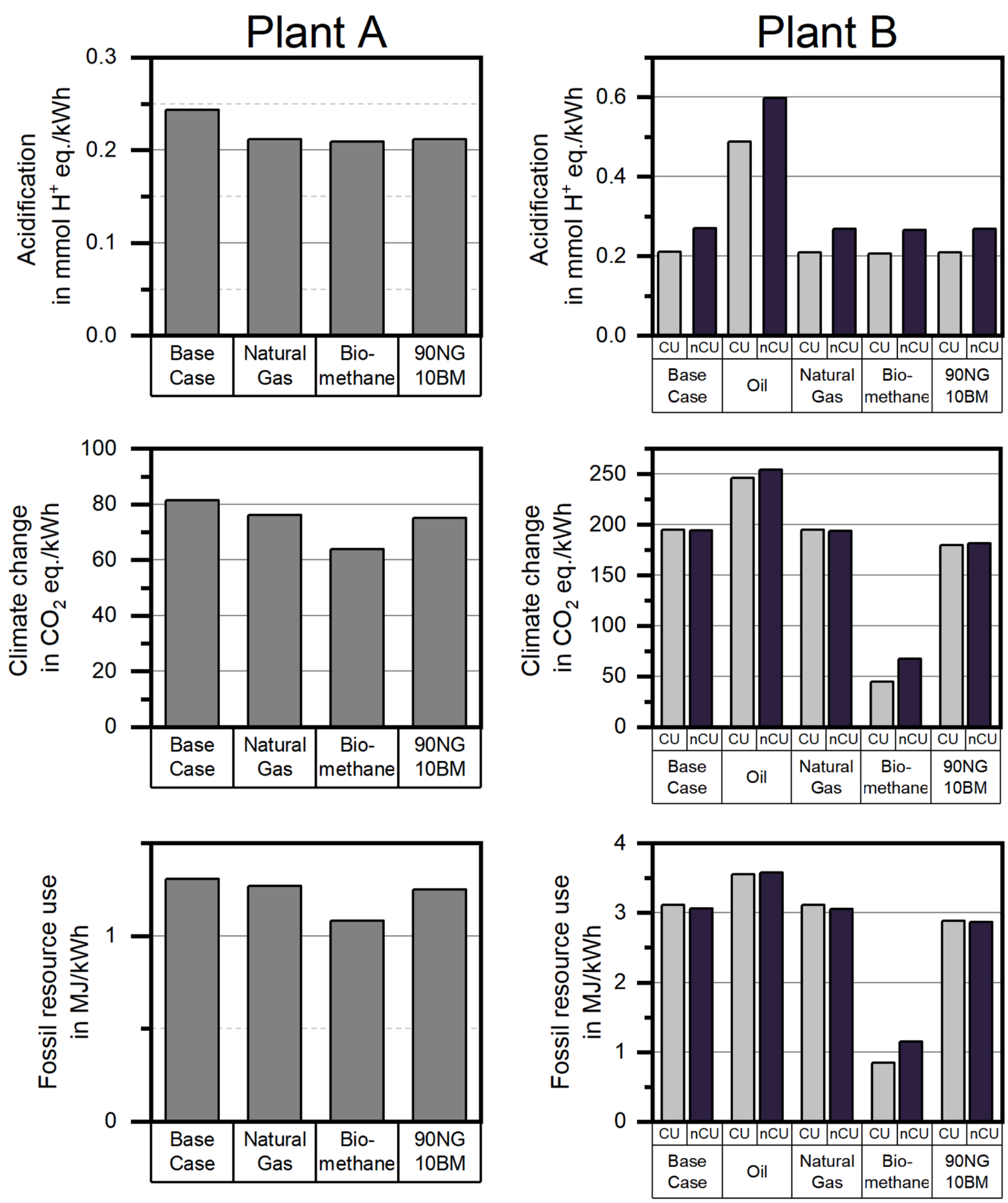

Fig. 6. LCA results of plant A (left column) and plant B (right column) for different peak load coverage: for plant B, the base case includes partly light fuel oil and mainly natural gas for peak load and redundancy and 100 % natural gas for the CU and for Plant A heating oil for peak load and redundancy. The other scenarios are natural gas, biomethane, and the realistic blend of 90 % natural gas and 10 % biomethane (90NG10BM). For Plant B, the results for using the CU (CU) and not using the CU (nCU) are shown for each scenario.

et al. (Wachsmuth et al., 2019) also suggested future scenarios in which the gas demand is covered mainly by e-methane and hydrogen. Other promising alternatives could be carbon-negative fuels, which are currently the focus of the European research project NET-Fuels (European Commission). This could be especially interesting when striving for the net zero per kWh in 2050 as per the taxonomy threshold (EU Technical Expert Group on Sustainable Finance, 2020).

3.3. Renewable electricity mix scenarios

In this section the influence of the electricity mix on the plants is investigated. Therefore, the base case using the German electricity mix (for the years 2005–2035 for plant A and 2011–2041 for plant B) is compared to applying the mostly renewable mix that's expected for the year 2050 (see Table 5 for details of the composition of the electricity mixes). In Fig. 7 the environmental impacts regarding ACI, CC and RUf are shown. For plant B the results are again depicted with and without the CU. Compared to the electricity mix of plant A and B which have a significant share of fossil-based energy (see Table 5), applying the electricity mix of 2050 leads to a reduction for every impact category. Whilst plant A is affected significantly by the change in electricity mix, the differences for plant B with the CU are much smaller. This can partly be attributed to the lower fossil shares in the mix for plant B (see Table 5). Applying the electricity mix of 2050, plant A demonstrates the greatest reduction in CC, achieving a 37 % decrease. Plant B can be reduced by 15 % in ACI at maximum when using the CU. However, without the CU, the mix has a greater impact since all electricity is obtained from the grid. As a result, without the CU, the largest reduction occurs in ACI with a decrease of 39 %. The electricity mix also has an effect on the evaluation of the CU use especially apparent in ACI: For the base case, the results would favor the use of the CU, while the use of the 2050 mix renders Plant B with the CU significantly less environmentally friendly. The difference between CU and nCU is even greater for the 2050 scenario for CC and RUf.

Although the electricity mix of 2050 still has a share of 18 % natural gas (see Table 5), the results reveal the potential of choosing an (location based) electricity contract with renewable energy.

With the results of scenario 2050 (49.5 g CO_2 eq./kWh) plant A comes close to the value 31.64 of the Genevan plant (Pratiwi and Trutnevyte, 2021) that uses low GWP hydro power to cover its electricity demand. Residual differences are mainly due to heating oil based peak load (in contrast to the supplementary heat with natural gas and waste incineration) and redundancy coverage and natural gas share in the 2050 electricity mix.

3.4. Limitations

While this study provides a comprehensive analysis based on current assumptions and data availability, several limitations and potential future developments must be taken into account in order to correctly interpret the results and their long-term relevance.

Firstly, the political landscape regarding the energy transition remains highly dynamic. Fluctuations in policy decisions—especially those related to the national energy mix, the regulation of fossil fuels, or the expansion of renewable energy—can substantially affect the viability and environmental performance of geothermal heating systems. Related to this is the uncertainty surrounding future standards for building insulation and the availability of subsidies for energy-efficiency measures, both of which can significantly influence heat demand and system sizing, yet were not varied in the current analysis.

Another important factor is climate change itself. This study assumes a moderate trajectory toward milder winters, which would reduce heating demand, and was implemented according to the projections by Kemmler et al. (Kemmler et al., 2020) (as detailed in Section 2.3.1). However, if the global average temperature increase exceeds 1.5 °C, regional climate effects may become more extreme or unpredictable, which could affect seasonal demand patterns.

The assumed system lifetime of 30 a also presents a limitation. While this value is commonly used for comparability in life-cycle assessments, many geothermal plants—particularly in the hydrothermal segment—can remain in operation significantly longer with proper maintenance and reinvestment. A longer operational period would improve the environmental performance per unit of heat delivered and may shift the relative importance of infrastructure impacts.

In terms of system operation, the assumed electricity demand for pumping was conservatively estimated based on existing technologies. Potential efficiency improvements or the integration of more advanced control systems were not accounted for, though they could lead to noticeable reductions in operational energy use over time.

Furthermore, infrastructure for peak load coverage was modeled using simplified assumptions. In reality, these systems are site-specific and may include a range of technologies such as gas boilers, electric

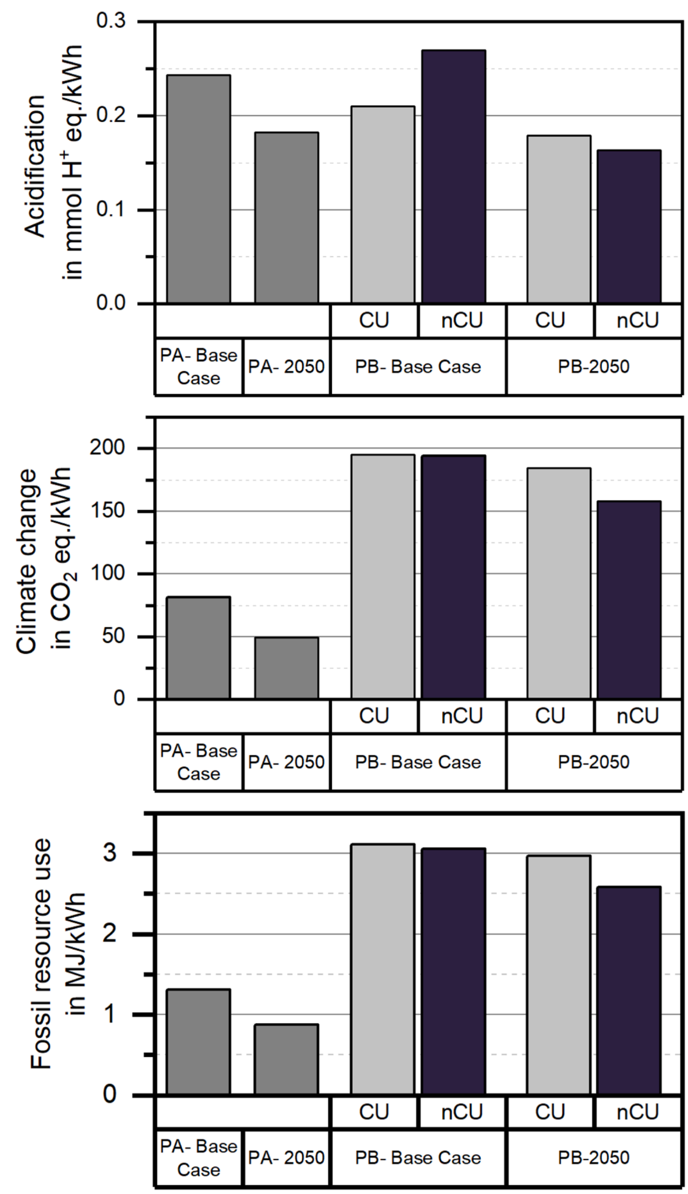

Fig. 7. LCA results for plant A (PA) and plant B (PB) on the categories ACI, CC and RUf for the Variation of the consumed electricity mix; comparison of the German electricity mix of the operational years to the mostly renewable mix in 2050 based on (Fattler et al., 2019) as well as scenarios with (CU) and without (nCU) the CU for plant B for each scenario.

heaters, or thermal storage. The choice of peak load technology can significantly influence the overall environmental balance, particularly with regard to emissions and fossil fuel dependency.

In addition, both the peak load demand and the electricity demand for system operation are based on measured data from recent years. For the purpose of this study, it is assumed that the relationship between electricity and fuel consumption and the total annual heat output remains constant in the future, reflecting historical trends. However, at the same time, a gradual increase in total heat output is assumed due to anticipated demand growth. This combination introduces a simplification, as it does not consider that such an increase could affect the operational efficiency or alter the proportion of auxiliary energy required. Factors such as scaling effects, system optimization, or shifts in user behaviourpl could lead to changes in the energy input per unit of heat delivered, which are not reflected in the current model. As a result, this assumption represents a potential source of uncertainty in the long-term projections.

Finally, it should be noted that all results are based on the current version of the ecoinvent database. As this database is regularly updated—especially with respect to electricity mixes, emission factors, and material flows—future versions may yield different results. This inherent dependence on data availability and representativeness limits the long-term reproducibility and transferability of the findings.

4. Conclusion

In this study, an LCA for two geothermal heating plants currently operating in the Southern German Molasse Basin was conducted. Thereby, the impact categories with highest relevance for the geothermal sector: ACI, CC, FET, HTC, HTNC, RUf and RUm were chosen according to (Parisi et al., 2020) as well as the method Environmental Footprint version 3.1 (Andreasi Bassi et al., 2023). All environmental impacts are related to the functional unit of 1 kWh net thermal energy including losses in the DHN as well as peak load and redundancy coverage. The environmental impact of the plants differ greatly between the categories since plant B has a greater share of heat provided by peak load boilers and a CU that is installed to cover electricity demand. Plant B also exhibits lower geothermal water temperatures than plant A. Furthermore, the year of commissioning of the plants differs, which affects the applied electricity mix. Plant A commenced operation in 2005, while plant B did so in 2011. The major contributor for almost all categories is the use of auxiliary energy with electricity consumption and peak load coverage by boilers. Therefore, scenarios varying the fuel used for peak load and the CU were analyzed. Considering heating oil, natural gas, and biomethane, it was apparent that biomethane has great potential for improving the environmental impact of plants, particularly when the peak load share is higher, such as in plant B. Plant A could benefit more by changing the electricity mix, from the German mix to the expected mix in 2050 by (Fattler et al., 2019) with a reduction of 39 % for CC-impact. These findings underline the importance of the energy transition to renewable sources, especially for deep geothermal heating plants.

Considering both reduction pathways (electricity mix and peak load coverage), plant B cannot fall below the EU's 100 g CO_2 eq./kWh taxonomy threshold (EU Technical Expert Group on Sustainable Finance, 2020) except for peak load scenarios with 100 % biomethane. This scenario may be feasible if the heating plant were situated near a biogas plant (with a converter) or if decentralized biomethane storage facilities were installed. However, neither of these options is feasible for this particular plant or many geothermal heating projects at present. Nonetheless, looking further into biomethane production pathways and further alternative fuel that might gain importance in the future such as hydrogen and e-Methane should be considered in future work. Although feasibility in production volume and costs have to be considered simultaneously.

Looking at a realistic scenario to improve Plant B, even when considering both the 2050 electricity mix and the realistic peak load scenario with 10 % biomethane and 90 % natural gas, the plant can only achieve a cumulative reduction of 14.2 % to 167.3 g CO_2 eq./kWh with the CU. Without the CU, a reduction of 25.3 % to 144.8 g CO_2 eq./kWh is possible. Therefore, it can be concluded that peak load coverage is crucial for heat plants with lower enthalpy sources. Considering thermal storages or high-temperature heat pumps (with a renewable electricity mix) or multiple drilling to cover the peak load entirely by geothermal sources could be highly beneficial and should be investigated in future work. DHN 4.0 with modern customer structures that do not require high temperatures are another way to ecologically improve plants like Plant B. This would minimize or eliminate the requirement for an additional temperature lift by the peak load boilers. However, it is important to acknowledge that not all locations are suitable for these DHN types, as modern buildings' infrastructure must be present.

In addition to the limitations and adjustment options just mentioned, this study clearly shows that deep geothermal heating plants are able to comply with the threshold of 100 g CO_2 eq./kWh (EU Technical Expert Group on Sustainable Finance, 2020). However, planning heating plants with less favorable geothermal sites requires careful consideration regarding auxiliary energy coverage. Additionally, it also proves the potential of the choice of auxiliary energy in terms of electrical energy mix and peak load coverage to effectively reduce the environmental impact and thus meet the objectives of ongoing GWP reductions until 2050 of the Technical Expert Group. Looking at the energy transition to renewable electricity production as well as innovative peak load technologies and the use of geothermal redundancy with multiple wells, future geothermal heating is a viable option for complying with the threshold value. The results of this study could be used as an incentive for the operators to switch to electricity contracts with renewable sources to further decrease the GWP and FRS.

CRediT authorship contribution statement

Hannah Uhrmann: Writing – review & editing, Writing – original draft, Visualization, Methodology, Investigation, Formal analysis, Conceptualization. **Florian Heberle:** Writing – review & editing, Supervision, Project administration, Funding acquisition. **Dieter Brüggemann:** Writing – review & editing, Supervision, Funding acquisition.

Declaration of competing interest

The authors declare that they have no known competing financial interests or personal relationships that could have appeared to influence the work reported in this paper.

Acknowledgments

Funded by the Deutsche Forschungsgemeinschaft (DFG, German Research Foundation) – 491183248. Funded by the Open Access Pub lishing Fund of the University of Bayreuth. Additionally, we gratefully acknowledge the Bavarian State Ministry of Science and Arts within the framework of the "Geothermal Alliance Bavaria" project for funding. Furthermore, Joshua Pohle is acknowledged for his contribution on the LCA-model for plant B.

Appendix

Table A.1
Results of the environmental impacts for the peak load scenarios for plant A per kWh.

	Base case	Natural gas	Biomethane	90NG 10BM
AA in mmol $H+$ eq.	0.243	0.212	0.209	0.211
CC in g CO_2 eq.	81.372	76.206	63.903	74.976
FE in CTUe	0.531	0.430	0.429	0.430
HTC in 10^{-11}•CTUh	6.227	5.741	5.611	5.728
HTNC in10^{-10}•CTUh	8.630	8.294	8.272	8.292
RUf in MJ	1.308	1.269	1.082	1.250
RUm in mg Sb eq.	0.497	0.481	0.486	0.481

Table A.2
Results of the environmental impacts for the peak load scenarios for plant B per kWh.

	Base case		Heating Oil		Natural gas		Biomethane		90NG 10BM	
	CU	nCU	CU	Ncu	CU	nCU	CU	nCU	CU	nCU
AA in mmol $H+$ eq.	0.210	0.270	0.488	0.598	0.208	0.268	0.206	0.266	0.208	0.268
CC in g CO_2 eq.	195.06	194.10	245.78	253.95	194.82	193.89	44.620	67.149	179.80	181.22
FE in CTUe	0.412	0.492	1.306	1.546	0.407	0.488	0.358	0.447	0.403	0.484
HTC in 10^{-11}•CTUh	7.192	7.813	10.758	12.154	7.151	7.797	5.808	6.664	7.016	7.683
HTNC in10^{-10}•CTUh	5.695	9.183	6.765	10.665	5.641	9.176	5.539	9.090	5.631	9.168
RUf in MJ	3.112	3.059	3.554	3.581	3.110	3.058	0.844	1.146	2.884	2.867
RUm in mg Sb eq.	0.275	0.540	0.261	0.537	0.270	0.540	0.366	0.620	0.280	0.548

Table A.3
Results of the environmental impacts for the electricity mix scenarios for plant A and B per kWh.

	Base case			2050		
	PA	PB-CU	PB-nCU	PA	PB-CU	PB-nCU
AA in mmol $H+$ eq.	0.243	0.210	0.270	0.182	0.179	0.163
CC in g CO_2 eq.	81.372	195.064	194.102	49.478	184.326	157.882
FE in CTUe	0.531	0.412	0.492	0.435	0.372	0.357
HTC in 10^{-11}•CTUh	6.227	7.192	7.813	6.195	6.751	6.323
HTNC in10^{-10}•CTUh	8.630	5.695	9.183	7.185	4.084	3.748
RUf in MJ	1.308	3.112	3.059	0.879	2.971	2.582
RUm in mg Sb eq.	0.497	0.275	0.540	0.554	0.159	0.149

Table A.4
LCI inputs for peak load coverage (Uhrmann et al., 2023).

Parameter	Description	Unit	Value	Source
Cruide oil/natural gas boiler	Aluminium, cast alloy	kg	557.05	(Eurostat, 2007; Wolf 2023)
	Steel, chromium steel 18/8, hot rolled	kg	24,880.17	(Eurostat, 2007; Wolf 2023)
	Stone wool, packed	kg	716.63	(Eurostat, 2007; Wolf 2023)
	Electricity, medium voltage	kWh	15,430.77	(Eurostat, 2007)
	Heat, district or industrial, natural gas	MJ	88,138.46	(Eurostat, 2007)
	Heat, district or industrial, other than natural gas	MJ	46,553.85	(Eurostat, 2007)
	Transport, freight, lorry 16–32 t, euro3	tkm	1307.69	(Eurostat, 2007)
	Transport, freight train	tkm	15,692.31	(Eurostat, 2007)
	Transport, freight, lorry 7.5–16 t, euro3	tkm	1307.69	(Eurostat, 2007)
Oil storage and catch basin	Oil storage, 3000l	p	140.60[a]	(Eurostat, 2007)
	Transport, freight, lorry 16–32 t, euro3	tkm	6896.55	(Eurostat, 2007)
	Transport, freight train	tkm	82,758.63	(Eurostat, 2007)
	Transport, freight, lorry 7.5–16 t, euro3	tkm	3416.82	(Eurostat, 2007)
Chimney	Chimney	m/kWh[b]	1.32E-07	(Eurostat, 2007)
	Transport, freight, lorry 16–32 t, euro3	tkm/kWh[b]	6.91E-07	(Eurostat, 2007)
	Transport, freight train	tkm/kWh[b]	8.29E-06	(Eurostat, 2007)
	Transport, freight, lorry 7.5–16 t, euro3	tkm/kWh[b]	3.29E-09	(Eurostat, 2007)
Heat production light fuel oil	Light fuel oil	kg/MJ[c]	2.57E-02	Operator
Heat production natural gas	Natural gas, high pressure[d]	m^3/MJ	2.87E-02	(Eurostat, 2007)
Heat production natural gas	Biomethane, high pressure[d,e]	m^3/MJ	2.87E-02	(Eurostat, 2007)

[a] : scaled to oil consumption for one year (4 GWh for 2019) according to (Eurostat, 2007).

[b] : scaled to total heat production through boilers according to (Eurostat, 2007).
[c] : MJ produced heat for peak load and redundancy, in total 81.6 GWh. Amount of fuel per MJ according to caloric values and degree of utilization.
[d] : the natural gas grids included proportionally in the dataset for natural gas and biomethane.
[e] :Composition of the biogas mix for conversion to biomethane taken from ecoinvent dataset of Switzerland.

Table A.5
LCI inputs for the district heating network of plant A (Uhrmann et al., 2023) and plant B.

Parameter	Description	Unit	Value		Source
			Plan A	Plant B	
Plastic sheath pipes	Steel, low-alloyed and drawing of pipes	kg/m DHN	15.27	45.08	(Biemann, 2015)
	Polyethylene, high density and extrusion, plastic pipes	kg/m DHN	4.43	11.33	(Biemann, 2015)
	Polyurethane, rigid foam	kg/m DHN	4.01	11.63	(Biemann, 2015)
	Tap water	kg/m DHN	17.68	66.96	(Biemann, 2015)
	Sand	kg/m DHN	243.32	774.96	(Biemann, 2015)
Connectors	Polyethylene, high density and Injection moulding	g/m DHN	164.37	702.53	(Biemann, 2015)
	Steel, low-alloyed and metal working	g/m DHN	502.04	2212.18	(Biemann, 2015)
	Polyethylene, high density and extrusion, plastic pipes	g/m DHN	136.54	374.24	(Biemann, 2015)
	Polyurethane, rigid foam	g/m DHN	100.73	367.08	(Biemann, 2015)
	Tap water	g/m DHN	165.44	1088.04	(Biemann, 2015)
	Sand	kg/m DHN	19.29	38.20	(Biemann, 2015)
Trench work	Welding: argon, liquid	g/m DHN	30.93	37.74	(Menberg et al., 2023)
	Welding:diesel, burned in diesel-electric generating set	MJ/m DHN	2.22	2.68	(Menberg et al., 2023)
	Bitumen adhesive compound, hot	kg/m DHN	152.97	820.86	(Menberg et al., 2023)
	Diesel, burned in building machine	MJ/m DHN	188.32	489.83	(Menberg et al., 2023)
	Waste asphalt	kg/m DHN	107.30	615.64	(Menberg et al., 2023)
Transport	Transport, freight, lorry >32 t	tkm/m DHN	51.35	41,125.88	(Menberg et al., 2023)
Transfer station	Steel, low-alloyed and drawing of pipes	kg/building	9.26	13.10	(Menberg et al., 2023)
	Steel, low-alloyed and metal working	kg/building	43.80	61.95	(Menberg et al., 2023)
	Stone wool, packed	kg/building	2.73	16.15	(Menberg et al., 2023)
	Steel, chromium steel and metal working	kg/building	19.25	75.05	(Menberg et al., 2023)
	Copper and metal working	kg/building	668.961	230.80	(Menberg et al., 2023)
	Polypropylene and polymer foaming	kg/building	1728.19	722.50	(Menberg et al., 2023)
Network pumps	Steel, low-alloyed and metal working	g/m DHN	22.64	183.96	operator

Table A.6
Results of the environmental impacts for the subsurface construction phase of plant A per kWh.

	Geothermal fluid cycle	Deep well pump	Well casing	Cementation	Drilling mud	Reservoir enhancement	Drill site preparation	Well head	Drilling rig drive
AA in mmol $H+$ eq.	4.37E-06	1.31E-06	1.35E-05	1.11E-06	6.30E-06	3.62E-07	3.26E-08	2.24E-07	8.66E-06
CC in g CO_2 eq.	6.53E-04	6.48E-05	2.63E-03	5.02E-04	1.17E-03	4.96E-05	3.92E-06	5.51E-05	6.90E-04
FE in CTUe	5.70E-03	1.38E-03	3.71E-02	4.54E-04	1.48E-02	7.01E-04	6.95E-06	1.26E-03	6.12E-04
HTC in 10^{-11}•CTUh	8.02E-12	1.64E-12	9.74E-11	4.63E-13	4.82E-12	3.91E-13	1.41E-14	3.55E-12	6.72E-13
HTNC in10^{-10}•CTUh	4.19E-12	1.17E-11	4.91E-11	3.18E-12	1.08E-11	7.54E-13	8.26E-15	8.16E-13	1.35E-12
RUf in MJ	1.39E-02	7.41E-04	2.79E-02	2.12E-03	1.32E-02	8.38E-04	4.77E-05	6.10E-04	8.94E-03
RUm in mg Sb eq.	2.73E-09	1.40E-08	5.36E-08	6.26E-10	1.84E-08	8.50E-10	1.72E-12	3.15E-10	2.97E-10

Table A.7
Results of the environmental impacts for the surface construction phase of plant A per kWh.

	Heat exchanger	Peak load and redundancy infrastructure	Building
AA in mmol $H+$ eq.	6.63E-07	2.01E-06	1.38E-06
CC in g CO_2 eq.	1.19E-04	2.37E-04	3.16E-04
FE in CTUe	9.31E-04	5.31E-03	4.84E-03
HTC in 10^{-11}•CTUh	1.90E-12	1.16E-11	1.31E-11
HTNC in10^{-10}•CTUh	1.85E-12	1.39E-11	4.50E-12
RUf in MJ	1.33E-03	2.63E-03	2.96E-03
RUm in mg Sb eq.	1.97E-09	1.53E-08	3.41E-09

Table A.8
Results of the environmental impacts for the district heating network construction phase of plant A per kWh.

	Plastic sheath pipes	Connectors	Trench work	Transport	Transfer station	Network pump
AA in mmol $H+$ eq.	9.31E-06	4.67E-07	2.69E-05	5.04E-07	1.21E-06	1.10E-08
CC in g CO_2 eq.	2.10E-03	1.10E-04	6.51E-03	1.56E-04	2.09E-04	2.70E-06
FE in CTUe	6.74E-02	2.37E-03	1.73E-02	5.36E-04	4.01E-03	6.19E-05
HTC in 10^{-11}•CTUh	1.04E-10	4.09E-12	2.49E-11	9.65E-13	9.66E-12	1.74E-13
HTNC in10^{-10}•CTUh	3.26E-11	1.42E-12	2.93E-11	1.46E-12	5.96E-12	4.00E-14
RUf in MJ	3.42E-02	1.82E-03	3.15E-01	2.26E-03	2.37E-03	2.99E-05
RUm in mg Sb eq.	1.74E-08	7.33E-10	7.65E-09	4.21E-10	4.08E-09	1.55E-11

Plan B.

Table A.9
Results of the environmental impacts for the subsurface construction phase of plant B per kWh.

	Geothermal fluid cycle	Deep well pump	Well casing	Cementation	Drilling mud	Reservoir enhancement	Drill site preparation	Well head	Drilling rig drive
AA in mmol $H+$ eq.	2.49E-06	5.39E-06	3.70E-07	2.74E-06	4.32E-07	1.82E-07	5.28E-07	9.70E-06	2.89E-07
CC in g CO_2 eq.	3.76E-04	1.05E-03	1.22E-04	4.84E-04	5.97E-05	4.46E-05	2.66E-05	7.73E-04	4.87E-05
FE in CTUe	3.23E-03	1.49E-02	4.03E-04	6.73E-03	8.33E-04	1.02E-03	5.51E-04	6.86E-04	2.73E-04
HTC in 10^{-11}•CTUh	4.57E-12	3.92E-11	1.75E-13	2.08E-12	4.72E-13	2.87E-12	6.58E-13	7.53E-13	5.02E-13
HTNC in10^{-10}•CTUh	2.44E-12	1.97E-11	8.63E-13	4.66E-12	9.12E-13	6.61E-13	4.67E-12	1.52E-12	4.09E-13
RUf in MJ	7.90E-03	1.12E-02	7.03E-04	5.60E-03	1.01E-03	4.93E-04	3.07E-04	1.00E-02	7.08E-04
RUm in mg Sb eq.	1.56E-09	2.14E-08	2.69E-10	7.52E-09	1.03E-09	2.55E-10	5.58E-09	3.33E-10	1.39E-10

Table A.10
Results of the environmental impacts for the surface construction phase of plant B per kWh.

	Heat exchanger	Peak load and redundancy infrastructure	Cogeneration unit	Building
AA in mmol $H+$ eq.	1.66E-06	1.38E-06	7.62E-08	1.67E-06
CC in g CO_2 eq.	2.81E-04	2.27E-04	1.86E-05	3.85E-04
FE in CTUe	1.81E-03	3.20E-03	4.24E-04	5.89E-03
HTC in 10^{-11}•CTUh	3.07E-12	7.27E-12	1.19E-12	1.59E-11
HTNC in10^{-10}•CTUh	3.78E-12	6.78E-12	2.75E-13	5.47E-12
RUf in MJ	3.11E-03	2.58E-03	2.06E-04	3.60E-03
RUm in mg Sb eq.	3.45E-09	7.37E-09	1.06E-10	4.15E-09

Table A.11
Results of the environmental impacts for the district heating network construction phase of plant B per kWh.

	Plastic sheath pipes	Connectors	Trench work	Transport	Transfer station	Network pump
AA in mmol $H+$ eq.	1.42E-05	9.57E-07	3.26E-05	3.23E-07	6.29E-07	4.76E-08
CC in g CO_2 eq.	3.19E-03	2.28E-04	7.92E-03	1.00E-04	1.07E-04	1.17E-05
FE in CTUe	1.04E-01	5.11E-03	2.08E-02	3.44E-04	1.67E-03	2.67E-04
HTC in 10^{-11}•CTUh	1.62E-10	9.44E-12	2.98E-11	6.19E-13	3.84E-12	7.51E-13
HTNC in10^{-10}•CTUh	5.03E-11	3.04E-12	3.56E-11	9.36E-13	2.85E-12	1.73E-13
RUf in MJ	5.11E-02	3.63E-03	3.83E-01	1.45E-03	1.22E-03	1.29E-04
RUm in mg Sb eq.	2.66E-08	1.53E-09	9.26E-09	2.70E-10	2.29E-09	6.68E-11

Data availability

Data will be made available on request.

References

Alberici S., Grimme W., Toop G. Biomethane production potentials in the EU: feasibility of REPowerEU 2030 targets, production potentials in the Member States and outlook to 2050. A Gas for Climate report. Utrecht, the Netherlands; 2022; Available from: https://www.europeanbiogas.eu/wp-content/uploads/2022/07/GfC_national-biomethane-potentials_070722.pdf. [December 05, 2023].

Andreasi Bassi, S., Biganzoli, F., Ferrara, N., Amadei, A., Valente, A., Sala, S., et al., 2023. Updated Characterisation and Normalisation Factors For the Environmental Footprint 3.1 Method. Publications Office of the European Union, Luxembourg. Available from. https://publications.jrc.ec.europa.eu/repository/handle/JRC130796 [December 26, 2023].

Bettgenhäuser K., Grözinger J., Petersdorff C., John A. Die Rolle von Gas im Zukünftigen Energiesystem.(in German). Köln; Available from: https://www.dvgw.de/medien/dvgw/forschung/berichte/g201802-201657.pdf. [November 05, 2023].

Biemann, K., 2015. Vergleichende Ökobilanzierung der semi- zentralen Hauswärmebereitstellung aus Holzreststoffen. Technischen Universität Darmstadt, GermanDarmstadt.

Bravi, M., Basosi, R., 2014. Environmental impact of electricity from selected geothermal power plants in Italy. J. Clean. Prod 66, 301–308. https://doi.org/10.1016/j.jclepro.2013.11.015.

DIN Deutsches Institut für Normung e.V, 2021. Environmental Management – Life cycle Assessment –Principles and Framework (ISO 14040:2021-02);13.020.10; 13.020.60 (14040:2021-02). Beuth Verlag GmbH, Berlin, D.

Douziech, M., Tosti, L., Ferrara, N., Parisi, M.L., Pérez-López, P., Ravier, G., 2021. Applying Harmonised Geothermal Life Cycle Assessment Guidelines to the Rittershoffen Geothermal Heat Plant. Energ. (Basel) 14 (13), 3820. https://doi.org/10.3390/en14133820.

EU Technical Expert Group on Sustainable Finance, 2020. Taxonomy: Final report of the Technical Expert Group on Sustainable Finance. Available from. https://finance.ec.europa.eu/system/files/2020-03/200309-sustainable-finance-teg-final-report-taxonomy_en.pdf [November 10, 2023].

European Commission. Increasing biomass conversion efficiency to carbon-negative sustainable biofuels by combination of thermal and bio-electrochemical processes: nET-Fuels. https://doi.org/10.3030/101083780.

European Commission. Communication from the Commission to the European Parliament, the Council, the European economic and Social Committee and the Committee of the regions: REPowerEU Plan. Brussels; 2022; Available from: http://energytransitionkorea.org/sites/default/files/2020-12/%ec%a7%80%ec%86%8d%ea%b0%80%eb%8a%a5%ed%88%ac%ec%9e%90%ec%a0%84%eb%9e%b5_sustainable%20europe%20investment%20plan.pdf. [December 17, 2023].

eurostat, 2023. Complete Energy balances: Germany - 2021 - fossil gasses. Available from. https://ec.europa.eu/eurostat/cache/infographs/energy_balances [November 20].

Fadel, M., Reinecker, J., Bruss, D., Moeck, I., 2022. Causes of a premature thermal breakthrough of a hydrothermal project in Germany. Geothermics 105, 102523. https://doi.org/10.1016/j.geothermics.2022.102523.

Faist Emmenegger, M., Heck, T., Jungbluth, N., Tuchschmid, M. (Eds.), 2007. Ecoinvent Data v2.0: Teil V: Erdgas. Swiss Centre for Life Cycle Inventories, German. Available from. www.ecoinvent.ch [February 28, 2023].

Faist-Emmenegger, M., Heck, T., Jungbluth, N., Tuchschmid, M. (Eds.), 2007. Ecoinvent Data v2.0: Teil V: Erdgas. Swiss Centre for Life Cycle Inventories. Available from. https://www.researchgate.net/profile/niels-jungbluth/publication/230725630_erdgas [February 28, 2023].

Fattler S., Conrad J., Regett A., Böing F., Guminski A., Greif S. et al. Dynamis - Hauptbericht: Dynamische Und Intersektorale Maßnahmenbewertung zur Kosteneffizienten Dekarbonisierung des Energiesystems. (in German); 2019; Available from: https://www.ffe.de/projekte/dynamis/. [December 15, 2023].

Fazio, S., Biganzioli, F., De Laurentiis, V., Zampori, L., Sala, S., Diaconu, E., 2018. Supporting Information to the Characterisation Factors of Recommended EF Life Cycle Impact Assessment methods: Version 2. from ILCD to EF 3.0, 2nd ed. Available from. https://publications.jrc.ec.europa.eu/repository/handle/jrc114822. [November 30, 2023].

Federal Network Agency Germany, 2023. Market Data Yearly Electricity Mix. Available from. https://www.smard.de/home [March 03].

Frick, S., Kaltschmitt, M., Schröder, G., 2010. Life cycle assessment of geothermal binary power plants using enhanced low-temperature reservoirs. Energy 35 (5), 2281–2294. https://doi.org/10.1016/j.energy.2010.02.016.

Gkousis, S., Harcouët-Menou, V., Damen, L., Welkenhuysen, K., Laenen, B., Compernolle, T., 2022a. Life cycle assessment of geothermal plants targeting the lower carboniferous limestone reservoir in northern Belgium. J. Clean. Prod 376, 134142. https://doi.org/10.1016/j.jclepro.2022.134142.

Gkousis, S., Thomassen, G., Welkenhuysen, K., Compernolle, T., 2022b. Dynamic life cycle assessment of geothermal heat production from medium enthalpy hydrothermal resources. Appl. Energy 328, 120176. https://doi.org/10.1016/j.apenergy.2022.120176.

Gkousis, S., Welkenhuysen, K., Compernolle, T., 2024. Integrated assessment of deep geothermal heating investments in Northern Belgium through techno-economic, life cycle, global sensitivity and real options analysis. Geothermics 121, 103027. https://doi.org/10.1016/j.geothermics.2024.103027.

Heberle, F., Schifflechner, C., Brüggemann, D., 2016. Life cycle assessment of Organic Rankine Cycles for geothermal power generation considering low-GWP working fluids. Geothermics 64, 392–400. https://doi.org/10.1016/j.geothermics.2016.06.010.

International Organization for Standardization, 2006. Environmental Management – Life cycle Assessment –Requirements and guidelines;13.020.10(14044:2006). Beuth Verlag GmbH, Berlin, D.

Karlsdottir, M.R., Heinonen, J., Palsson, H., Palsson, O.P., 2020. Life cycle assessment of a geothermal combined heat and power plant based on high temperature utilization. Geothermics 84, 101727. https://doi.org/10.1016/j.geothermics.2019.101727.

Keim M., Hamacher T., Loewer M., Molar-Cruz A., Schifflechner C., Ferrand T. et al. Bewertung Masterplan Geothermie. (in German); 2020; Available from: https://geothermie-allianz.de/wp-content/uploads/2022/09/Gutachten-Masterplan-Geothermie-Bayern.pdf. [December 20, 2023].

Kemmler A., Kirchner A., Maur A auf der, Ess F., Kreidelmeyer S., Piégsa A. et al. Energiewirtschaftliche Projektionen und Folgeabschätzungen 2030/2050: Dokumentation von Referenzszenario und Szenario mit Klimaschutzprogramm 2030 10. März 2020.(in German); 2020; Available from: https://www.bundesregierung.de/breg-de/service/publikationen/energiewirtschaftliche-projektionen-und-folgeabschaetzungen-2030-2050-1730266. [December 20, 2023].

Lauf T., Memmler M., Schneider S. Emissionsbilanz Erneuerbarer Energieträger: Bestimmung der Vermiedenen Emissionen im Jahr 2022.(in German). Dessau-Roßlau; 2023a; Available from: https://www.umweltbundesamt.de/sites/default/files/medien/11850/publikationen/20231219_49_2023_cc_emissionsbilanz_erneuerbarer_energien_2022_bf.pdf. [December 15, 2023].

Lauf T., Memmler, M., Schneider S. Emissionsbilanz Erneuerbarer Energieträger: Bestimmung der Vermiedenen Emissionen im Jahr 2022. German. Dessau-Roßlau; 2023b; Available from: https://www.umweltbundesamt.de/sites/default/files/medien/11850/publikationen/20231219_49_2023_cc_emissionsbilanz_erneuerbarer_energien_2022_bf.pdf. [August 15, 2024].

Li, J., Tarpani, R.R.Z., Gallego-Schmid, A., Stamford, L., 2024. Life cycle assessment of repurposing abandoned onshore oil and gas wells for geothermal power generation. Sci. Total. Env. 907, 167843. https://doi.org/10.1016/j.scitotenv.2023.167843.

Li, J., Tarpani, R.R.Z., Stamford, L., Gallego-Schmid, A., 2023. Life cycle sustainability assessment and circularity of geothermal power plants. Sustain. Prod. Consum 35, 141–156. https://doi.org/10.1016/j.spc.2022.10.027.

Maar, L., Seifermann, S., 2023. Assessing the Environmental Sustainability of Deep Geothermal Heat Plants. Energ. (Basel) 16 (19), 6774. https://doi.org/10.3390/en16196774.

McCay, A.T., Feliks, M.E.J., Roberts, J.J., 2019. Life cycle assessment of the carbon intensity of deep geothermal heat systems: a case study from Scotland. Sci. Total. Env. 685, 208–219. https://doi.org/10.1016/j.scitotenv.2019.05.311.

Menberg, K., Heberle, F., Bott, C., Brüggemann, D., Bayer, P., 2021. Environmental performance of a geothermal power plant using a hydrothermal resource in the Southern German Molasse Basin. Renew. Energy 167, 20–31. https://doi.org/10.1016/j.renene.2020.11.028.

Menberg, K., Heberle, F., Uhrmann, H., Bott, C., Grünäugl, S., Brüggemann, D., et al., 2023. Environmental impact of cogeneration in binary geothermal plants. Renew. Energy 218, 119251. https://doi.org/10.1016/j.renene.2023.119251.

Milligan, G., Wood, G., Younger, P., Feliks, M., Mccay, A., Gillespie, M., et al., 2016. Hill of Banchory Geothermal Energy Project Feasibility Study Report en. BanchoryAvailable from: https://eprints.gla.ac.uk/118526/ [December 10, 2023].

Oliver-Solà, J., Gabarrell, X., Rieradevall, J., 2009. Environmental impacts of the infrastructure for district heating in urban neighbourhoods. Energy Policy 37 (11), 4711–4719. https://doi.org/10.1016/j.enpol.2009.06.025.

Ortner S., Pehnt M., Over, Margarete, Blömer, Sebastian, Ochse S., Ziegler R., Bohn K. et al. Dekarbonisierung Von Energieinfrastrukturen: Ein politischer Unterstützungsrahmen für das Beispiel Wärmenetze. (in German). Dessau-Roßlau; 2023; Available from: https://www.umweltbundesamt.de/sites/default/files/medien/479/publikationen/cc_08-2023_dekarbonisierung_von_energieinfrastrukturen.pdf. [March 05, 2023].

Parisi, M.L., Douziech, M., Tosti, L., Pérez-López, P., Mendecka, B., Ulgiati, S., et al., 2020. Definition of LCA Guidelines in the Geothermal Sector to Enhance Result Comparability. Energ. (Basel) 13 (3534), 1–18. https://doi.org/10.3390/en13143534, 13.

Paulillo, A., Cotton, L., Law, R., Striolo, A., Lettieri, P., 2020. Geothermal energy in the UK: the life-cycle environmental impacts of electricity production from the United Downs Deep Geothermal Power project. J. Clean. Prod 249, 119410. https://doi.org/10.1016/j.jclepro.2019.119410.

Pehnt M., Weiß U., Fritz S., Jessing D., Lempik J., Mellwig P. et al. Evaluation Des Erneuerbare-Wärme-Gesetz (EWärmeG): Endbericht im Auftrag des Ministeriums für Umwelt, Klima und Energiewirtschaft Baden-Württemberg. (in German). Heidelberg, Berlin, Freiburg, Karlsruhe, Rottenburg; 2018; Available from: https://www.ifeu.de/fileadmin/uploads/2018_ifeu-et-al._Evaluation-des-Erneuerbare-W%C3%A4rme-Gesetz-EW%C3%A4rmeG_final_akt_Verz.pdf. [12.12.23].

Pratiwi, A., Ravier, G., Genter, A., 2018. Life-cycle climate-change impact assessment of enhanced geothermal system plants in the Upper Rhine Valley. Geothermics 75, 26–39. https://doi.org/10.1016/j.geothermics.2018.03.012.

Pratiwi, A.S., Trutnevyte, E., 2021a. Life cycle assessment of shallow to medium-depth geothermal heating and cooling networks in the State of Geneva. Geothermics 90, 101988. https://doi.org/10.1016/j.geothermics.2020.101988.

Pratiwi, A.S., Trutnevyte, E., 2021b. Life cycle assessment of shallow to medium-depth geothermal heating and cooling networks in the State of Geneva. Geothermics 90 (Suppl), 101988. https://doi.org/10.1016/j.geothermics.2020.101988.

Rogge, S., 2003. Geothermische Stromerzeugung in Deutschland - Ökonomie, Ökologie und Potenziale. Technische Universtät Berlin, GermanBerlin, D.

Rossi, F., Zuffi, C., Parisi, M.L., Fiaschi, D., Manfrida, G., 2023. Comparative scenario-based LCA of renewable energy technologies focused on the end-of-life evaluation. J. Clean. Prod 405, 136931. https://doi.org/10.1016/j.jclepro.2023.136931.

Uhrmann, H., Heberle, F., Brüggemann, D., 2022. Life Cycle Assessment of an operating geothermal heat project in the Southern German Molasse Basin. In: European Geothermal Congress 2022: Berlin, Germany, 17-21 October 2022 proceedings. EGEC. In: Bundesverband Geothermie, European Geothermal Energy Council, Brussels, pp. 1–9.

Uhrmann, H., Heberle, F., Brüggemann, D., 2023. Life Cycle Assessment and Scenario Analyses of an Operating Geothermal Heat Project in the Southern German Molasse Basin. In: Smith, J.R. (Ed.), 36th International Conference on Efficiency, Cost, Optimization, Simulation and Environmental Impact of Energy Systems (ECOS 2023). Las Palmas De Gran Canaria, Spain. ECOS 2023, pp. 2992–3001.

Wachsmuth J., Michaelis J., Neumann F., Degünther C., Köppel W., Zubair A. Roadmap Gas für die Energiewende – Nachhaltiger Klimabeitrag des Gassektors. (in German). Dessau-Roßlau; 2019; Available from: https://www.umweltbundesamt.de/publikationen/roadmap-gas-fuer-die-energiewende-nachhaltiger. [December 16, 2023].

Wang, Y., Du, Y., Wang, J., Zhao, J., Deng, S., Yin, H., 2020. Comparative life cycle assessment of geothermal power generation systems in China. Resour. Conserv. Recycl. 155, 104670. https://doi.org/10.1016/j.resconrec.2019.104670.

Wolf. Planungsunterlage: Großkessel 450-5200 kW. (in German); Available from: https://www.wolf-heiztechnik.at/Downloads/Planungsunterlagen. [December 12, 2023].

Zhang, R., Wang, G., Shen, X., Wang, J., Tan, X., Feng, S., et al., 2020. Is geothermal heating environmentally superior than coal fired heating in China? Renew. Sustain. Energy Rev. 131, 110014. https://doi.org/10.1016/j.rser.2020.110014.

Zuffi, C., Manfrida, G., Asdrubali, F., Talluri, L., 2022. Life cycle assessment of geothermal power plants: a comparison with other energy conversion technologies. Geothermics 104, 102434. https://doi.org/10.1016/j.geothermics.2022.102434.